

POLYMER DEGRADATION IN SLIDING
ELASTOHYDRODYNAMIC LUBRICATION

A THESIS

Presented to

The Faculty of the Division of Graduate
Studies and Research

By

David L. ^{Leary} Walker

In Partial Fulfillment
of the Requirements for the Degree
Master of Science in Mechanical Engineering

Georgia Institute of Technology

November, 1973

ACKNOWLEDGMENTS

The author would like to express his appreciation to the members of his committee for their help and guidance throughout this investigation. The advice and assistance of the chairman, Dr. D. M. Sanborn, is particularly appreciated. Dr. W. O. Winer's guidance in the fluid analysis stage is gratefully acknowledged.

Special thanks are extended to Dr. C. L. Liotta for his guidance in analysis of certain fluids.

The author is indebted to Dow Corning Corporation and Rohm and Haas Company for their services in analyzing fluid samples. The research reported here was supported by the National Science Foundation (NSF GK-31154).

Finally, the author would like to thank his wife, Maureen, for her patience and understanding, for without her this study would not have been completed.

TABLE OF CONTENTS

	Page
ACKNOWLEDGMENTS.	ii
LIST OF TABLES	iv
LIST OF ILLUSTRATIONS.	v
NOMENCLATURE	vii
SUMMARY.	ix
Chapter	
I. INTRODUCTION.	1
Reasons for Investigation	
Previous Studies	
Objectives	
II. TEST FLUIDS	6
III. EHD EXPERIMENTAL PROCEDURE.	9
Equipment	
Technique	
IV. DETERMINATION OF MOLECULAR WEIGHT	25
Viscosity Measurements	
Analytical Techniques	
V. EXPERIMENTAL RESULTS.	34
Silicones	
Other Synthetics	
Organic Hydrocarbons	
General	
VI. DISCUSSION OF RESULTS	66
VII. CONCLUSIONS	70
VIII. RECOMMENDATIONS	72
APPENDIX A	73
BIBLIOGRAPHY	76

LIST OF TABLES

Table		Page
1.	Test Fluids.	7
2.	Elastohydrodynamic Operating Conditions.	23
3.	Energy Input Into the Fluids	24
4.	Summary of Experimental Results.	35
5.	Apparent and Permanent Viscosity Loss.	68

LIST OF ILLUSTRATIONS

Figure	Page
1. Schematic Diagram of Experimental Equipment.	10
2. Sapphire Configuration	11
3. Interferometer	14
4. Schematic Diagram of Locater Mechanism	16
5. Sapphire Hole Location Sequence.	18
6. Time Variation of Temperature, h_c , and TC.	21
7. Schematic Diagram of Microcapillary.	27
8. Molecular Weight Distribution, Fluid S6.	38
9. Molecular Weight Distribution, Fluid S6.	39
10. Molecular Weight Distribution, Fluid S6.	40
11. Molecular Weight Distribution, Fluid S6.	41
12. Molecular Weight Distribution, Fluid S7.	43
13. Molecular Weight Distribution, Fluid S8.	44
14. Molecular Weight Distribution, Fluid P2.	47
15. Molecular Weight Distribution, Fluid P2.	48
16. Molecular Weight Distribution, Fluid P2.	49
17. Molecular Weight Distribution, Fluid P2.	50
18. Molecular Weight Distribution, Fluid P2.	51
19. Molecular Weight Distribution, Fluid P3.	52
20. Molecular Weight Distribution, Fluid P3.	53
21. Molecular Weight Distribution, Fluid P3.	54
22. Molecular Weight Distribution, Fluid P3.	55

Figure		Page
23.	Molecular Weight Distribution, Fluid P3.	56
24.	Molecular Weight Distribution, Fluid P6.	57
25.	Molecular Weight Distribution, Fluid P6.	58
26.	Molecular Weight Distribution, Fluid P6.	59
27.	Molecular Weight Distribution, Fluid P6.	60
28.	Molecular Weight Distribution, Fluid P6.	61
29.	Energy Input Versus Degradation and Viscosity Loss	63
30.	Energy Input per Unit Volume Versus Degradation and Viscosity Loss	65

NOMENCLATURE

Å	Angstrom
C	Polymer solids concentration (weight percent)
C_c	Capillary constant
D	Capillary diameter (inches)
E	Energy input rate into the fluid (kcal/cm sec)
EHD	Elastohydrodynamic
GC	Gas chromatography
GPC	Gel permeation chromatography
K	Unit constant
L	Length of capillary (inches)
MW	Molecular weight (atomic units)
MWD	Molecular weight distribution
PAMA	Polyalkymethacrylate
ΔP	Pressure differential (pounds per square inch)
R	Capillary radius (inches)
S	Viscosity loss
TC	Traction coefficient
V	Volume (cubic inches)
au	Atomic unit
h	EHD film thickness (inches)
k	Refractive index
n	Interference fringe order
e	Energy input into the fluid (kcal/gmole)

$\dot{\gamma}$	Shear rate (sec^{-1})
λ	Wavelength of light (\AA)
μ	Lubricant viscosity (cs)
τ	Shear stress (dynes/cm^2)
$\Delta\phi$	Net phase shift of interfering ray

Subscripts

a	Apparent viscosity loss
b	Base oil
c	Centerline
e	Effective
i	Initial
m	Maximum
n	Number average
o	Original fluid
p	Permanent
s	Sheared fluid
v	Viscosity average
w	Weight average

SUMMARY

This investigation is a study of polymer degradation in sliding elastohydrodynamic lubrication. Elastohydrodynamic lubrication is typically found in highly loaded point contacts such as gears, certain cams and followers and rolling element bearings. The lubricant in this contact is subjected to extremely high pressures (150,000 psi) and very high shear rates (10^6 sec^{-1}). A variety of fluids were examined. These included bulk polymer lubricants, hydrocarbon lubricants, and polymer containing hydrocarbon solutions.

A technique was developed that allows small samples (10 microliters) of the test fluid to be extracted directly from the elastohydrodynamic contact. These samples were then analyzed to determine changes in viscosity and molecular weight distribution.

Severe degradation was found in fluids which had molecular weights of over 1000. This degradation resulted in viscosity losses of up to 70 percent. It is concluded that a designer should assume the base oil viscosity when designing mechanisms which are to use polymers containing hydrocarbon mixtures. When designing for bulk polymers each combination of fluid and mechanism should be tested.

CHAPTER I

INTRODUCTION

Multigrade motor oils have come into widespread use in recent years. These oils are basically a mixture of a low viscosity base oil and a small percentage of a high molecular weight additive which has the effect of increasing the viscosity of the oil at all temperatures and decreasing the effect of temperature on viscosity. Ideally this would give effective lubrication when the engine is hot while not being so viscous at low temperatures that it would cause difficulty in starting. These additives (viscosity index improvers) and other high molecular weight polymers are known to degrade (break down into lower molecular weight molecules) when they are subjected to mechanical shearing. This shearing is the result of the relative motion of the bearing surfaces which the oil lubricates. When this degradation occurs in an engine the remaining lubricant may no longer meet its original specifications [1,2]¹ nor be capable of proper lubrication since the thickness of the fluid film which separates the bearing surfaces is a function of the oil viscosity. For this reason polymer degradation has become a problem of concern to lubricant

¹Numbers in brackets designate references at end of thesis.

manufacturers and users.

The increasing use of high molecular weight synthetic lubricants by industry in locations where stable, clean fluids are required has created a need for more information on the stability of these fluids when subjected to mechanical shearing.

The most extreme conditions of mechanical shearing that a lubricant must withstand are those found in elastohydrodynamic lubrication (EHD). Some aspects of EHD lubrication are as yet not well understood but this type of lubrication has been extensively studied in recent years [3,4,...15]. In EHD lubrication a thin fluid film (on the order of 10^{-5} inches) separates the bearing surfaces and sustains loads which cause normal surface stresses ($>10^5$ psi) that are sufficient to deform the surfaces elastically. The shear rates (velocity gradients) experienced by the fluid range up to 10^7 sec^{-1} . EHD lubrication is typically found in rolling element bearings, certain cam followers and gears.

These conditions result in energy input rates into the fluid on the order of 10^7 kcal per gmole. This can be compared to an activation energy of 80 kcal per gmole of carbon-carbon bonds. Although the fluid is usually subjected to these conditions for only a short period of time (less than 1.0 millisecc) some degradation can be expected.

Previous Studies

In previous studies the problem of mechanically induced polymer degradation has been approached in either of two ways: (1) attempts have been made to simulate actual conditions on laboratory apparatus, or (2) tests have been done using production equipment.

By testing on a specially designed apparatus, the conditions under which the degradation takes place are usually well defined. Some of the simulators in use at this time are: capillaries, concentric cylinders, high speed stirring, ultrasonic shearing, and various methods of spraying and shaking. These methods have been extensively reviewed by Casale, Porter and Johnson [16] recently and will be only briefly discussed here.

Degradation by shearing in capillaries is probably the oldest method used [16,17]. In this type apparatus the fluid is forced through a capillary (a small diameter tube or orifice). The shear stress experienced by the fluid can be calculated using Poiseuille's equation. The major disadvantages of this method are the inhomogeneous shear field (varying from a maximum at the wall to zero at the centerline) and the fact that many passes through the capillary are usually necessary to reach an equilibrium molecular weight.

The concentric cylinder arrangement was designed so that a uniform shear field could be applied to the test

fluid long enough for it to reach an equilibrium molecular weight [18,19]. In these devices the fluid is sheared in the annular gap between the two cylinders by rotating one of the cylinders. Shear rates up to 10^6 sec^{-1} have been reported [18]. The other methods mentioned are highly dependent on apparatus design and are not widely used.

None of these test procedures is capable of reaching the extreme conditions of pressure and shear stress that are present in EHD lubrication. Therefore tests in production machinery have been necessary. This type of test can be exemplified by tests run on multigrade motor oil in automotive engines [1,2]. The engine is set up on a dynamometer with the test oil acting as a lubricant and is run for a specified period of time. The viscosity of the oil is then checked to determine if the viscosity index improver is still effective. If there is a change in the effect of the viscosity index improver, this indicates degradation of the polymer. This type of testing yields good qualitative results, however, the conditions on the fluid when the polymer degrades are practically impossible to determine. These conditions range from EHD lubrication at the cam follows and gears to low shear stirring in the sump with temperature ranges from ambient at the start of the test to over 200°F after warmup.

Objective

The objective of this study was to subject a variety of fluids to conditions that are found in EHD lubrication and determine the extent of polymer degradation. The test fluids were subjected to pressure of up to 150,000 psi and shear rates of approximately 10^6 sec^{-1} . Samples of the fluids were collected and analyzed to determine if degradation had occurred. The viscosity of the sheared fluids was measured and the viscosity average molecular weight was calculated using available empirical equations [20,21]. If this method resulted in an indication of degradation, further analysis was done using gel permeation chromatography [22], flame ionization spectroscopy and other analytical methods. These results were then correlated with polymer type, concentration, shear rate and energy input rate to the fluid.

CHAPTER II

TEST FLUIDS

The lubricants selected for examination were chosen so that a wide range of molecular weights and fluid types could be tested. Detailed descriptions of the test fluids are given in Appendix A and summarized in Table 1.

As representative examples of the hydrocarbon type fluids, a paraffinic base oil and three solutions of high molecular weight polyalkylmethacrylate (PAMA) were chosen. Two of these solutions used a PAMA additive with a viscosity average molecular weight (MW_v) of 560,000 atomic units (au) with concentrations of four and eight percent. The third solution used a PAMA additive with a MW_v of 1,650,000 au and a concentration of four percent. In this manner variations with concentration and MW could be studied. The paraffinic base oil with an average MW of 404 was also tested as a control.

Six synthetic fluids were tested. A commercially available silicone diffusion pump fluid with a MW of 546 au was tested because of its very narrow MW distribution. Because of this property small variations in MW could be detected. Another commercially available silicone lubricant which had a bimodal MW distribution centered around MWs of

Table 1. Test Fluids²

Designation ³	Fluid Description
P1	Paraffinic base oil (R-620-12)
P2	P1 + 4% polyalkylmethacrylate (PL-4521)
P3	P1 + 8% polyalkylmethacrylate (PL-4521)
P6	P1 + 4% polyalkylmethacrylate (PL-4523)
S1	Diester-Plexol 201 bis-2-ethyl hexyl sebacate (PL-5159)
S5	Pentaphenyltrimethyltrisiloxane (DC-705)
S6	Dimethylsiloxane (DC-200)
S7	Dimethylsiloxane Blend (E1923-48)
S8	Dimethylsiloxane Blend (E1923-49)
S9	Modified Polyphenyl Ether (MCS-418)

²Manufacturer's designation is shown in parentheses. See Appendix A for detailed description.

³The fluid designations correspond to designations used in previous studies on these fluids [12].

16,000 and 47,000 au was tested. The results obtained with this fluid (see section on silicone fluids) led to tests of two silicone blends with widely dispersed MW distributions. Both of these blends were dimethylsiloxanes but in one, trihydroxyl groups had been substituted as end-block radicals. These fluids were selected to determine if there is some MW below which no degradation occurs and also if the different end-block radicals had an effect on degradation (see section on silicone fluids).

Two further types of synthetic lubricants were tested, a sebacate with a MW of 426 au and a modified polyphenyl ether with an average MW of 423. The sebacate diester is a commonly used lubricant in jet engines where high temperature stability is required. The polyphenyl ether is an experimental lubricant which shows promise for applications which require oxidation and radiation stability.

CHAPTER III

EHD EXPERIMENTAL PROCEDURE

Experimental Equipment

In order to study the EHD contact, the apparatus shown in Figure 1 was used. This is a modification of an apparatus described in a previous publication by D. M. Sanborn [12]. The EHD contact is formed by rotating the steel sphere about an axis parallel to the surface of the sapphire while normally loading it against the sapphire. A synthetic sapphire was selected for a bearing surface because of its adequate elasticity, strength and transparency.

The higher elasticity of the sapphire insures that most of the elastic deformation will take place in the steel bearing surface. The initial sapphire disc used in this study was 0.187 inches in diameter, approximately 0.030 inches thick and had a small hole (approximately 0.003 inches in diameter) in its center (Figure 2). A disc 0.310 inches in diameter, 0.060 inches thick with a hole approximately 0.002 inches in diameter was used in the later tests. Several methods of drilling small holes were attempted. Laser drilling was tried but available lasers were not capable of the small clean holes needed for this research.

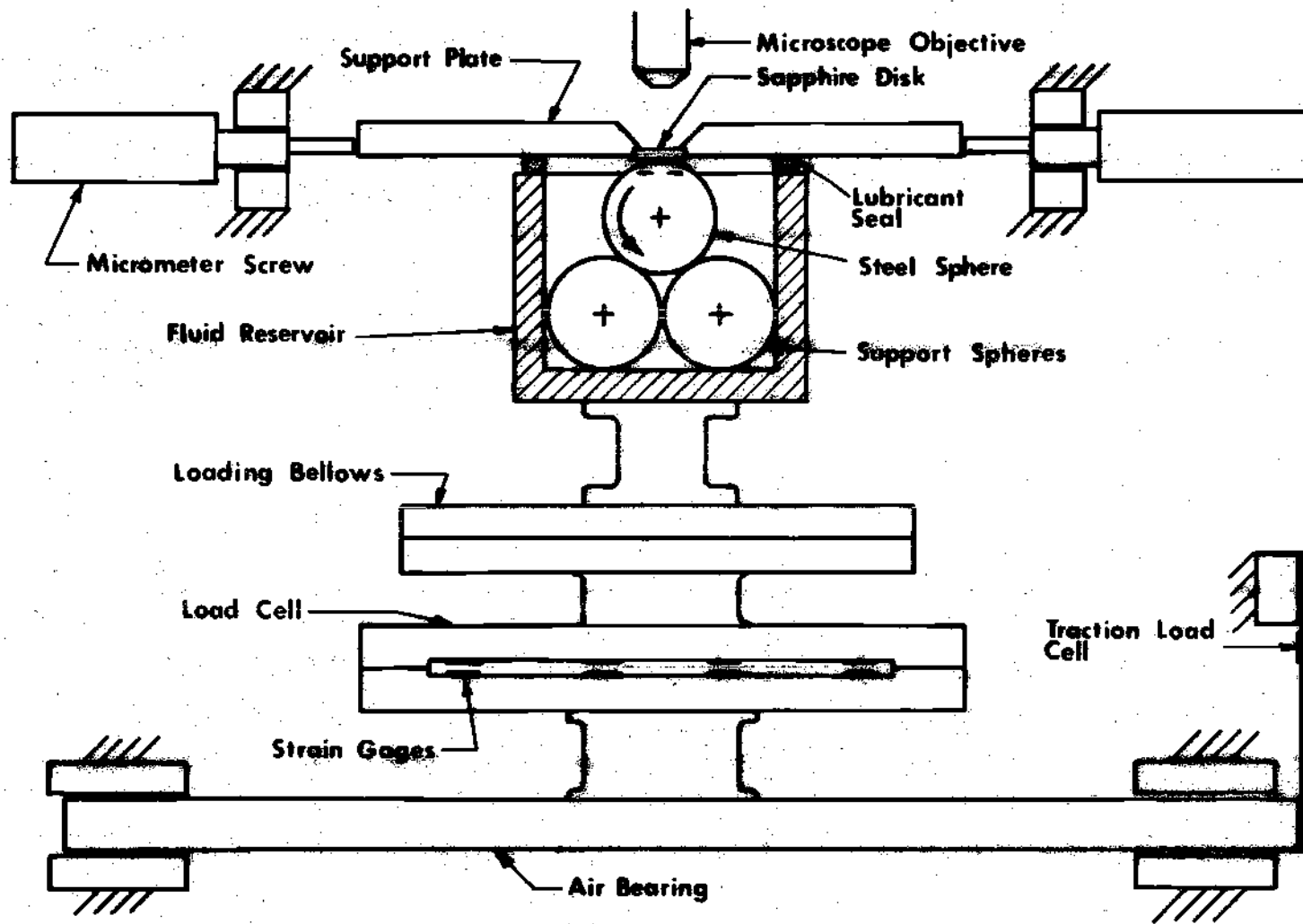
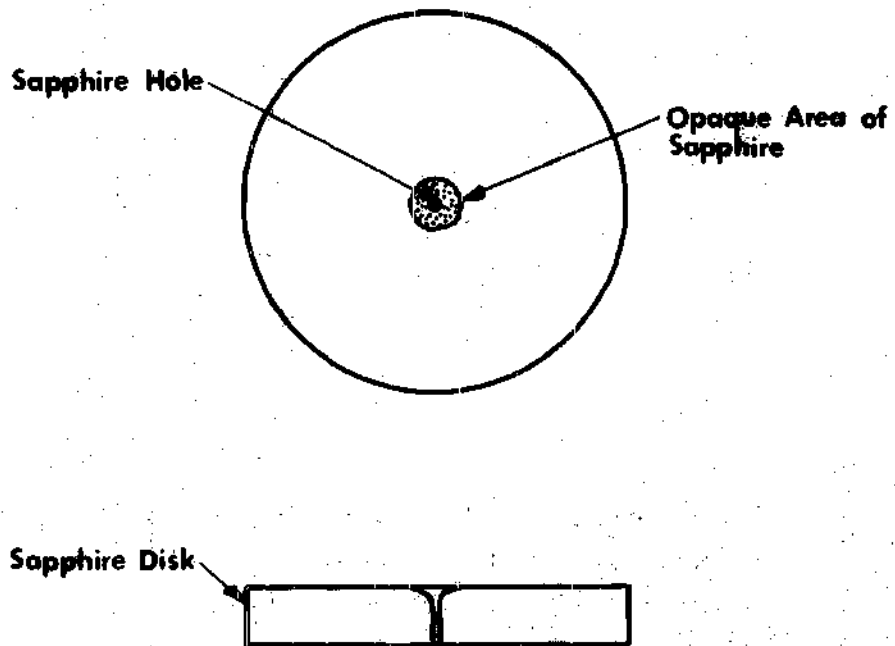


Figure 1 Schematic Diagram of the Experimental Equipment



Note: See Text for Dimensions

Figure 2 Sapphire Configuration

Ultra-sonic drilling was found to be possible but too costly. The holes used were drilled using proprietary techniques that are used in industry for making diamond wire drawing dies. The shape and angle of the hole cannot be precisely controlled using this technique (see Figure 2 for general shape), however, it is possible to see through the hole during testing for alignment purposes as is explained in the experimental procedure section. The conical shape of the hole did block part of the contact zone from view.

The lower bearing surface was a chromium steel ball 1.25 inches in diameter with a surface finish of 1.5 micro-inches (rms). This sphere was rotated through a flexible coupling cemented to its surface. It was supported and loaded against the sapphire by three similar steel spheres which were rigidly fitted into an aluminum cube which also forms the oil reservoir (see Figure 1). For tests over a long period of time (up to two hours) a seal was fitted between the sapphire mount and the oil reservoir as shown in order to reduce leakage and thus insure an adequate supply of oil. For shorter tests this seal was removed so that it would not interfere with the action of the air bearing needed for traction measurements. The normal load was applied by pressurizing a bellows located below the oil reservoir. This load was measured with the strain gage array as shown in Figure 1 [12,13,14].

An optical interference technique was used to determine

the film thickness [11,12]. The basic components of the interferometer are shown in detail in Figure 3. They are: the sapphire, the lubricant, and the steel sphere. The interference of the two reflected rays A and B in Figure 2 are almost totally responsible for the observed interference patterns. Basic theory of interferometry [23] predicts that bright interference fringes will appear whenever

$$h = \frac{\lambda}{2k} \left(n + \frac{\Delta\phi}{2\pi} \right); n = 0, 1, 2, \dots$$

and dark fringes whenever

$$h = \frac{\lambda}{2k} \left(n + \frac{\Delta\phi}{2\pi} - 1/2 \right); n = 0, 1, 2, \dots$$

The term $\Delta\phi$ represents the net phase shift due to reflections between rays A and B in Figure 3. The constant k is the refractive index of the fluid. The value of λ in the equations is the wavelength of the incident light in air. The light used was not strictly monochromatic since it was obtained using a tungsten light source and a 5340 Å Schott interference filter having a band width of 220 Å. The value 5340 Å was used for λ [12].

The resulting interference fringe patterns were observed and photographed through a Leitz metallurgical microscope using a magnification factor of 100X. The observed contact area was 0.015 inches in diameter for the

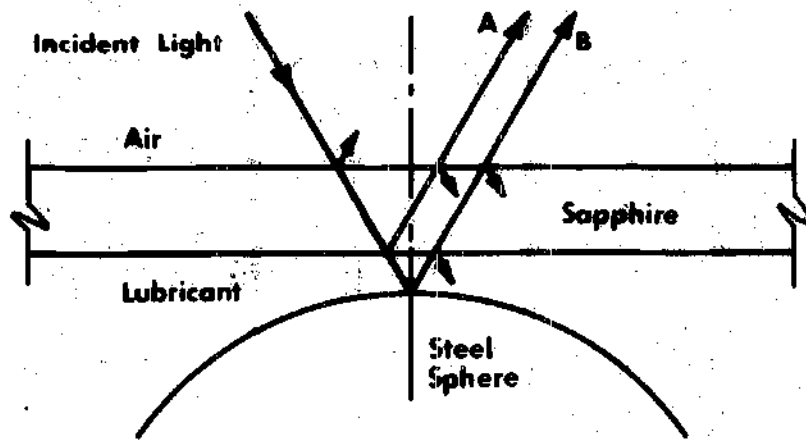


Figure 3 Interferometer

load of 15 pounds used throughout this study. The vertical illuminator of the microscope was used to direct incident light onto the EHD contact. Photographs were taken at intervals during the experiments as a record of the exact location of the hole in the sapphire relative to the contact zone. These photographs were taken using a standard Polaroid attachment and black and white film.

The oil samples were taken by moving the sapphire and using the microscope to optically align the sapphire hole in the center of the exit region of the contact (see experimental procedure section). The sapphire and its mounting plate were moved in a direction parallel to the axis of rotation of the sphere by means of an eccentric locator (see Figure 4). Location perpendicular to the axis of rotation was accomplished with a set of opposing micrometer screws.

In order to determine the energy input rate into the fluid, the force transmitted by the fluid perpendicular to the normal force (i.e. the traction force) must be known. This was measured by allowing the entire loading assembly to move in the air bearings as shown in Figure 1. The force was measured by a strain gage array attached to a restraining cantilever load cell as shown.

Experimental Technique

The tests run on each fluid were carried out following the procedure outlined below:

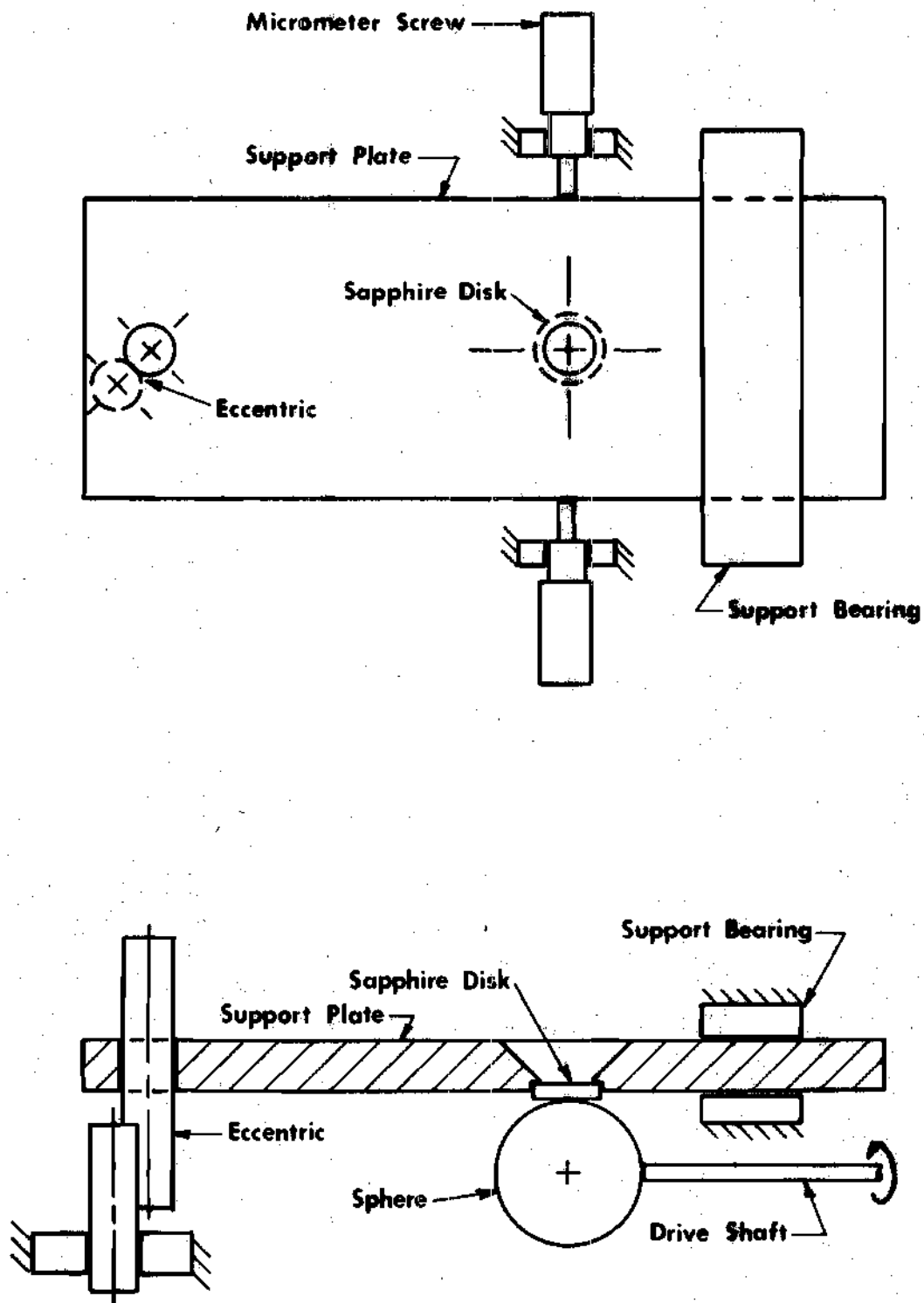


Figure 4 Schematic Diagram of Locator Mechanism

(1) After careful cleaning several times with xylene and acetone, the oil reservoir was filled with the fluid to be tested, the reservoir seal was installed as needed and the air bearing was not in operation.

(2) The sapphire was then checked to be sure it was parallel with the sphere supports. This was done by applying a nominal load to the ball with the ball stationary and noting the size of the contact. The diameter of the EHD contact is indicative of the contact load. The load was then released and the sapphire moved to a different location where the load was again applied and the contact size checked. The attitude of the sapphire was adjusted until the contact size was constant. This procedure insured that the load would remain constant when the sapphire was moved.

(3) The magnitude of the load was then set by adjusting the pressure applied to the bellows. The load was read on an oscilloscope which had previously been calibrated along with the strain gage array.

(4) The sapphire was moved into a position such that the 0.003 inch diameter hole would be in the wake formed by the contact (see Figure 5). It was found that in this position no oil would flow upward through the hole. In fact, any oil on top of the sapphire would be drawn down into the oil reservoir.

(5) With the load at zero, the speed control of the direct current motor was set for a given ball surface velocity

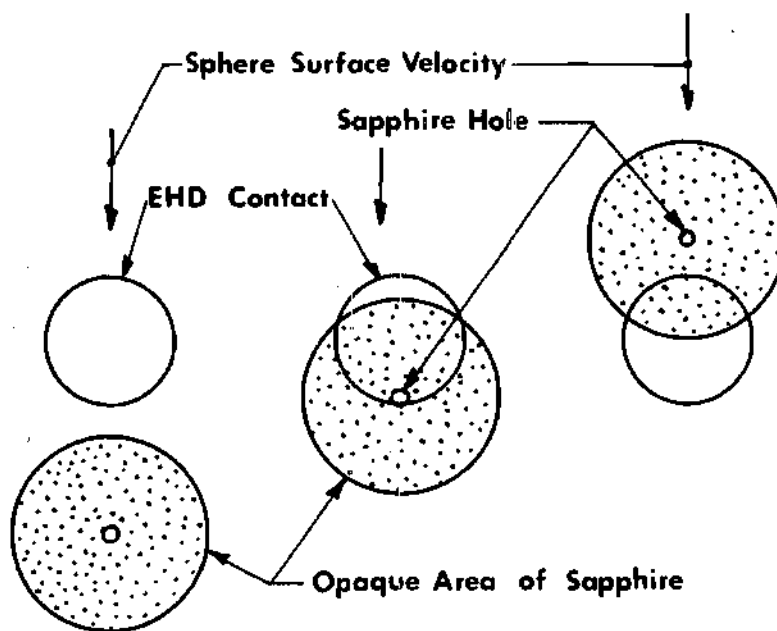


Figure 5 Sapphire Hole Location Sequence

(92.1 inches per second was used for most tests). The predetermined load was then applied.

(6) Using the eccentric locator (see Figure 4), the sapphire hole was aligned directly behind the center of the contact zone (see Figure 5).

(7) The sapphire was then moved with the micrometer screws until there was an indication of oil flow into the hole. This indication usually took the form of a blacking-out of the hole as seen through the microscope, generally occurring when the hole was three-quarters to fully into the contact zone. This estimate of a depth of penetration into the EHD contact was made by assuming that the contact zone would be essentially unchanged by the presence of the hole. The visible front edge of the contact was used to establish the location of the EHD contact boundary (see Figure 5).

(8) When a sufficient amount of oil had collected on the sapphire, two ten microliter samples were extracted using a Microtrol disposable bore syringe. The samples were marked for identification and one was sealed for later analysis.

(9) The machine was stopped and the sapphire hole was moved forward to the EHD contact inlet. A small vacuum pump was used to remove excess oil from the sapphire. The same procedure was used to start the apparatus and a sample was taken from the entrance region of the contact zone.

Further control samples were taken from the oil

reservoir and the original fluid sample container.

For measuring the traction coefficient (traction force divided by the normal force) and film thickness, a similar procedure was followed through step five with the following exceptions: (1) the reservoir seal was not used; (2) the air bearing was in operation; and (3) a similar sapphire with no hole was used.

The time required to collect enough fluid for a sample varied with each fluid but was usually around two hours. Locating the sapphire hole such that oil flow was assured took up to one hour. After a positive indication of flow through the hole, it was usually an hour before enough oil had been collected for a sample to be taken. This varied with the flow rate of oil through the contact and the position of the sapphire hole.

During an experiment, the temperature of the oil in the reservoir increased by about thirty degrees Fahrenheit. Since this change in temperature affects the fluid properties, and, therefore, may alter the operating parameters, a two hour test was made in which the temperature and traction force were recorded (see Figure 6). The temperature was measured with a copper-constantan thermocouple placed between the three support spheres in the lubricant supply. Photographs were also taken at selected time intervals for film thickness calculation. The film thickness data points are shown. From the ten minute point on the TC data had a

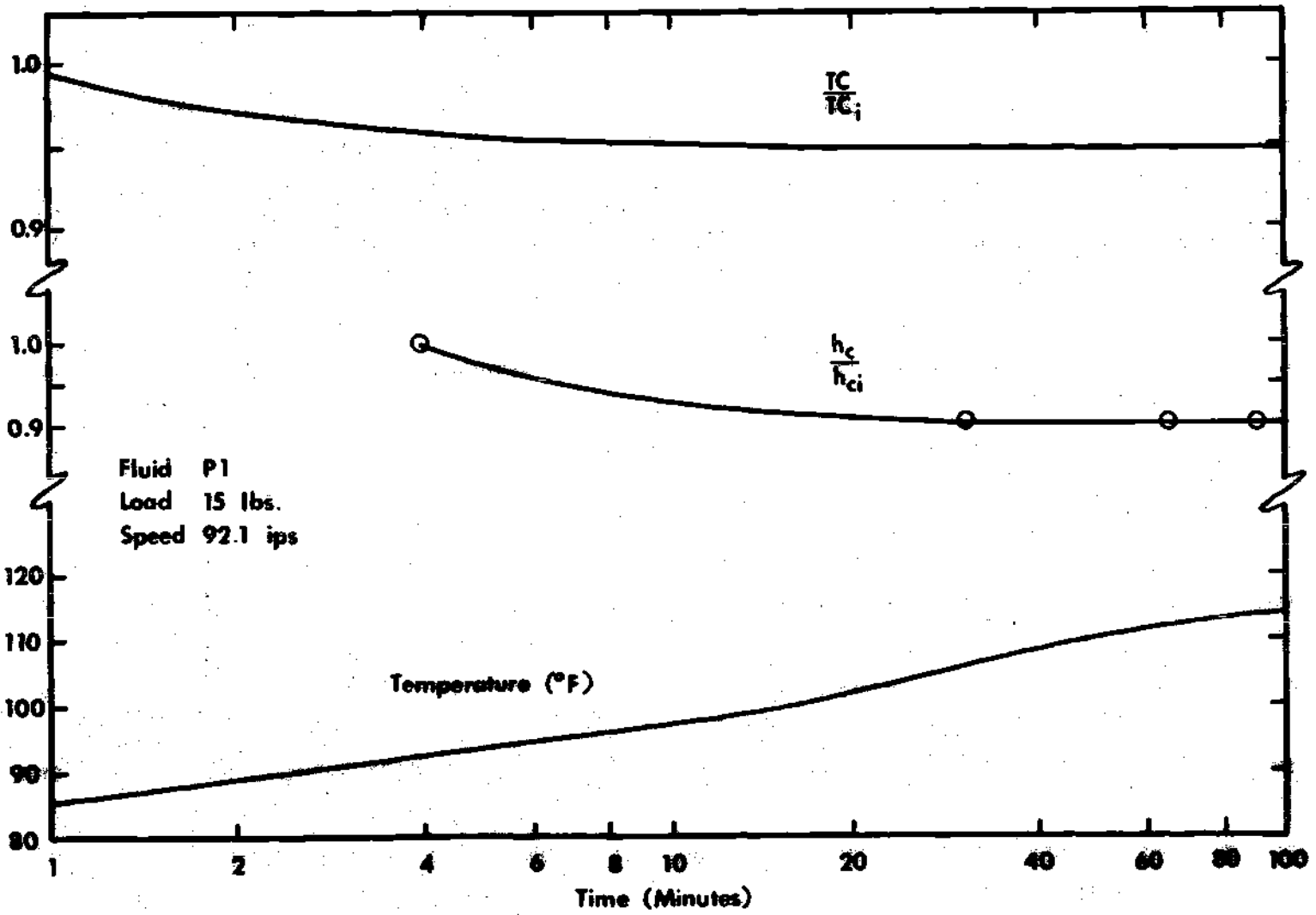


Figure 6 Time Variation of Temperature, h_c and TC

standard deviation of 0.03. It was determined that the traction and film thickness did not change appreciably (more than 5%) during this period. The apparatus is not presently capable of closer control of the temperature.

The experimental conditions of each test are given in Table 2. Also listed are the centerline film thickness and the traction coefficient (t_c) measured at ten minutes into a test. Table 3 is a summary of the average conditions experienced by the fluid in the EHD contact. An average shear rate, γ , is determined from the relative velocity of the bearing surfaces divided by the film thickness. The average shear stress, τ , is calculated by dividing the traction force by the contact area. The energy dissipation rate per unit volume (E) is given by the product of the shear stress and the shear rate. Finally, the energy dissipation rate per gram mole of polymer (ϵ) is obtained by multiplying the dissipation rate per unit volume by the volume and the average molecular weight and dividing by the mass flow rate and for the mixtures the weight concentration of polymer solids.

The traction coefficient and film thickness appear inversely in the equations for energy dissipation in the film. The variation of these quantities (TC and h_c) shown in Figure 6 results in a variation of less than 5 percent in the energy dissipated.

Table 2. Elastohydrodynamic Operating Conditions

Fluid	M_o cs (77°F)	Load lb	Speed ips	h_c $\times 10^6$ in	TC
P1	52	14.7	92.8	8.6	0.035
P2	112	15.0	92.1	9.8	0.033
P3	274	15.0	92.1	12.3	0.032
P6	240	15.0	92.1	9.9	0.038
S1	17.2	15.0	92.1	3.7	0.024
S5	175	15.6	57	17	0.068
S6	931	15.6	95	10	0.027
S7	1200	15.0	92.1	7.3	0.035
S8	1060	15.0	92.1	8.0	0.033
S9	56	15.0	92.1	11.8	0.042

Table 3. Energy Input Into the Fluids

Fluid	$\gamma \times 10^{-6}$ sec ⁻¹	$\tau \times 10^{-6}$ dynes/cm ²	$E \times 10^{-3}$ $\frac{\text{kcal}}{\text{cm}^3 \text{sec}}$	$e \times 10^{-9}$ $\frac{\text{kcal}}{\text{gmole}}$
P1	10.7	252	68.5	6.08
P2	9.4	248	50.4	258,000.0
P3	7.5	230	43.9	99,500.0
P6	9.3	274	63.7	536,000.0
S1	25.0	173	109.8	10.2
S5	3.4	490	42.3	8.1
S6	9.5	194	46.9	465.0
S7	12.6	252	80.7	98.8
S8	11.5	238	69.4	298.0
S9	7.8	302	60.0	5.6

CHAPTER IV

DETERMINATION OF MOLECULAR WEIGHT

A variety of techniques were used to analyze the samples obtained from the EHD contact. The viscosity of most of the fluids was measured in a micro capillary. Where possible and necessary, further analysis was done using gel permeation chromatography, gas chromatography, flame ionization spectroscopy, infrared absorption spectroscopy and mass spectroscopy.

Viscosity Measurements

Due to the small sample size (10 μ l) the only standard method of viscometry that could be used was plate and cone viscometry. This method was tried using a Haake Rotovisco with a plate and cone attachment (PKII). This procedure was satisfactory for the base hydrocarbon oil (P-1); however, it was not satisfactory for the non-Newtonian fluids. At the rotational speeds necessary to be within the range of this instrument; the shear rates (900 sec⁻¹) approached those where the fluids are entering their second Newtonian regions [24]. However, the MW viscosity correlations which were used to estimate degradation are applicable only to the low shear viscosity.

In order to overcome these deficiencies, a glass

capillary viscometer was developed and used.

From the Hagen-Poiseuille equation, the viscosity, μ , of a fluid is given by [25]

$$\mu = \frac{\pi D^4 (\Delta P) t}{K V L}$$

where D is the capillary diameter

L is the capillary length

ΔP is the pressure drop across the capillary

V is the volume passing through the capillary

t is the time required, and

K is a constant for a given set of units.

For a given capillary with a constant volume, this equation reduces to:

$$\mu = C_c \Delta P t$$

where C_c is the capillary constant. This form of the equation was used for calibration and viscosity calculations.

No commercially available capillary viscometers were found which could measure the small sample size so one was made (Figure 7). The micro capillary was made by heating a glass tube and pulling it down to the approximate size needed. The original tube was 3.5 inches long, 0.04 inches outside diameter and 0.02 inches inside diameter. The tube was heated in its center over a length of approximately 0.75

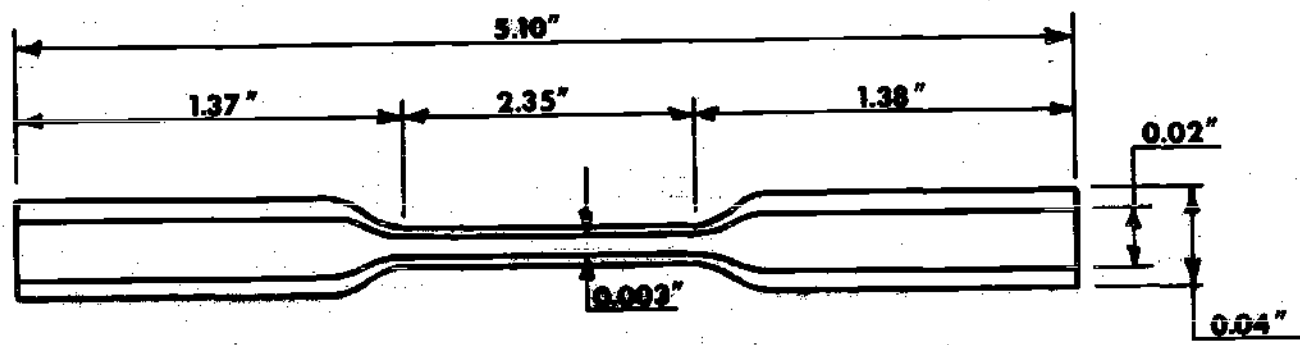


Figure 7 Schematic Diagram of Microcapillary

inches. This section was pulled down to a capillary 2.35 inches long and 0.003 inches inside diameter. This capillary was then cemented inside a larger diameter glass tube for strength. A glass tube with a 90° bend was fastened to each end of the capillary. The entire assembly was placed in a constant temperature bath with the capillary in a horizontal position. The bent tubes were connected to a manometer which was used to apply a pressure differential across the capillary. A water manometer was used for all measurements except the high viscosity silicone in which case a mercury manometer was used. The water manometer was constructed of polyvinylchloride tubing and distilled water. The manometer was connected to the capillary with small diameter surgical tubing. Using this method there was a small amount of leakage in the pressure applied to the fluid through the tubing connections. This was accounted for by taking the average of pressure readings at the beginning and end of each measurement. Maximum leakage was 0.15 inches of water with a 10 inches pressure differential. Gravity effects due to minor deviations of the capillary from the horizontal were corrected by taking the average of measurements made in both directions through the capillary. Ten measurements were normally made for a single fluid sample.

The combination of PVC tubing and water displayed a hysteresis effect [26] which gave pressure readings 0.1 inches of water too high. This error was corrected by

subtracting this amount from all readings.

The effects of the meniscus in each end of the capillary tube cancel each other. This will always be the case unless the contact angle at the air-liquid-solid interface is greater than zero for one meniscus which can only occur when the liquid does not wet the solid. This hysteresis effect typically occurs with a low surface energy solid and a high surface energy liquid, such as polyvinylchloride and water. All the fluids tested in this study have zero contact angles with glass [26]. In order to insure that wetting did occur, the samples were passed through the capillary before any measurements were made. Experimental repeatability was obtained by taking viscosity measurements with different pressure differentials on a fluid. Any unbalanced pressure drop across the meniscus will be a constant error in the measurements. With pressure differentials of one to ten inches of water on test fluid S-60, no measurable error was found.

The procedure used with the micro capillary was:

- (1) The capillary tube was carefully purged with xylene and acetone and checked under a microscope to be sure it was free of contamination.

- (2) Approximately 5 μ l of sample was drawn into the capillary tube. The bent tubes were then connected to the capillary tube.

- (3) This entire assembly was fastened to a support

plate and placed in a constant temperature bath. The bath temperature was held at $210^{\circ} \pm 0.1^{\circ}\text{F}$ for the hydrocarbon solutions; $77^{\circ} \pm 0.2^{\circ}\text{F}$ for the silicone fluids (these temperatures correspond to those required for the MW-viscosity correlations); and $100^{\circ}\text{F} \pm 0.2^{\circ}\text{F}$ for the sebacate and the polyphenylether. The temperatures were measured with a calibrated mercury-in-glass thermometer.

(4) After allowing 30 minutes for temperature equilibrium, the bent tubes were connected to the manometer. The fluid was forced through the capillary in order to insure wetting.

(5) A pressure was set with the manometer and recorded.

A stop watch was used to record the time necessary for one meniscus to travel between two standard marks on the support plate. A second pressure reading was taken and the pressure differential was removed. At no time was either meniscus allowed to pass the joints at the capillary tube ends nor enter the reduced portion of the capillary.

The capillary was calibrated at regular intervals with a viscosity standard (fluid S-60 supplied by Cannon-Instrument Co.) at all temperatures where measurements were made. One calibration was done using the standard fluid S-2000 by the same supplier as a cross check.

To insure that differences in fluid type did not influence the measurement, a relatively large (10 ml)

unsheared sample of each fluid was taken from the original container and its viscosity was measured in a routine glass viscometer which was also calibrated with standard fluid S-60. This sample was then measured in the micro capillary.

If the capillary constant was not identical with that found with the standard fluid, the constant $C_c = \frac{\mu}{\Delta P t}$ derived using the similar fluid, was used for the sheared samples except for the methacrylate mixtures. These high MW polymers are easily broken down and may degrade even in the mild shearing conditions of the viscometer. The capillary constant varied a maximum of 1% with the PAMA fluids.

The shearing forces acting on the fluid are maximum at the capillary wall and may be estimated by [25]

$$\tau_w = \frac{\Delta P}{4(L/D)} \text{ (psi)}$$

where ΔP is the pressure differential across the fluid in psi,

L is the capillary length (in inches) and

D is the capillary diameter in inches.

The maximum shear rate is given by [25]

$$\dot{\gamma} = \frac{\Delta P R}{2\mu L} \text{ (sec}^{-1}\text{)}$$

where μ is the viscosity in reyns.

The maximum shear stress and shear rates applied to any fluid

in the capillary were 0.00183 psi ($126 \frac{\text{dynes}}{\text{cm}^2}$) and 70 sec⁻¹ respectively. The normal operating conditions in the capillary for the low viscosity fluids (all except the silicones) gave shear stresses on the order of $10 \frac{\text{dynes}}{\text{cm}^2}$.

These viscosities were then used to calculate the viscosity average molecular weight. For the silicone fluids, the following relation was used [20]:

$$\log_{10} \mu = 1.00 + 0.0123 \sqrt{MW_v}$$

where μ is the viscosity in centistokes at 25°C and MW_v is the viscosity average molecular weight.

For the PAMA solutions, the following relation was used [21]:

$$\mu = \mu_B [1.03 + 1.328 \times 10^{-5} (C)^{1.25} (MW_v)^{0.818} \exp(-0.294 \mu_B^{0.5})]$$

where μ is the viscosity of the blend in centistokes, at 210°F,

μ_B is the viscosity of the base oil in centistokes, at 210°F,

C is the polymer solids concentration in weight percent, and

MW_v is the viscosity average molecular weight.

Other Analytical Techniques

Several other analytical techniques were employed in order to give more specific information about the MW distribution before and after shearing in the EHD contact.

For the higher polymers (PAMA and silicones), Gel Permeation Chromatography) was employed to get a MW distribution. Gas Chromatography, Infra-Red Spectroscopy, or Mass Spectroscopy were used with the lower MW fluids.

Gel Permeation Chromatography (GPC) and Gas Chromatography (GC) employ the same principle to separate the components of a mixture. The sample is mixed with a carrier fluid (usually benzene for GPC and helium for GC) and is passed through a column which contains a network of particles (typically polystyrene beads in GPC and liquid coated ceramic in GC) to which the sample fluid adsorbs. This adsorption is a function of concentration and MW. As the carrier fluids pass through the column, components having the various MWs become separated. As the carrier fluid exits from the column variations in the mixture are detected. The variation in refractive index of the solution is commonly used in GPC. Variations in thermal conductivity or flame ionization spectrometry is used with GC.

Infra-red spectroscopy measures the adsorption by the fluid of infra-red radiation. Mass spectroscopy ionizes the molecules and by acceleration into a magnetic field determines approximate molecular weights.

Infra-red and mass spectroscopy can give indications of any new species present in the solution as would be the case if crosslinking occurred in some of the low MW fluids. However, neither of these techniques give reliable data on changes in relative composition.

CHAPTER V

EXPERIMENTAL RESULTS

The results of the tests are shown in Table 4. In this table each fluid is listed twice, the subscript, o, indicates the original fluid and the subscript, s, indicates the sheared fluid. The first two columns are the measured viscosity and the percentage change in viscosity. The changes throughout Table 4 are calculated by subtracting the sheared quantity from the original and dividing by the original. The second two columns are the calculated viscosity average molecular weights and the percentage change in MW_v . The fifth and sixth columns are the weight average MWs as determined by GPC and the change in this quantity. The seventh column is the number average MW also determined by GPC. This quantity is highly dependent upon the extremely high MW fractions in some of the test fluids and has the greatest possible error. The final column is the dispersity as calculated by dividing the weight average MW by the number average MW and is a measure of the spread of MWs found in the sample.

Silicones

With the low MW fluid S5, no degradation was detectable. This fluid was tested using a gas chromatograph with a

Table 4. Summary of Experimental Results

Fluid	μ (cs)	$\Delta\mu$ %	MW _V	Δ MW _V %	MW _W	Δ MW _W %	MW _N	MW _W /MW _N
P1 _O	31.2		404		---	---	---	---
P1 _S	30.7 ⁴	1.6	404	0.0	---	---	---	---
P2 _O	12.97		560,000		610,000		140,000	4.5
P2 _S	7.49 ⁵	42.3	155,000	72.3	220,000	64	66,000	3.5
P3 _O	27.24		560,000		770,000		150,000	5.1
P3 _S	10.56 ⁵	61.0	111,000	80.2	160,000	79	23,000	6.7
P6 _O	30.62		1,650,000		3,200,000		390,000	8.3
P6 _S	8.08 ⁵	73.6	146,000	91.2	230,000	93	68,000	3.4
S1 _O	11.41		426		---	---	---	---
S1 _S	11.9 ⁶	-4.3	---	---	---	---	---	---
S5 _O	175		---		546		---	---
S5 _S	---	---	---	---	546	0.0	---	---
S6 _O	931		26,000		45,600		10,300	
S6 _S	409 ⁷	56.1	17,400	33.0	28,000	38.6	9,280	3.0

continued

Table 4. (Concluded)

Fluid	μ (cs)	$\Delta\mu$ %	MW_V	ΔMW_V %	MW_W	ΔMW_W %	MW_N	MW_W/MW_N
S7 _o	1200	---	---	---	43,000	---	4,150	---
S7 _s	---	---	---	---	---	---	---	---
S8 _o	1060	---	---	---	160,000	---	---	---
S8 _s	---	---	---	---	---	---	---	---
S9 _o	29.1	---	---	---	422	---	---	---
S9 _s	29.3 ⁶	-0.7	---	---	424	-0.4	---	---

⁴ Measured at 100°F with Rotovisco.

⁵ Measured at 210°F with micro capillary.

⁶ Measured at 100°F with micro capillary.

⁷ Measured at 77°F with micro capillary.

thermal conductivity detector. The chromatographs of the silicone fluids were made by Dow Corning Corporation, the manufacturer of these fluids. No viscosity measurements were made on this fluid because there was not enough sample collected in the original test to perform these measurements and the original fluid was not sufficient to duplicate the test at a later date.

Fluid S6 exhibited marked degradation after shearing in the EHD contact. Both viscosity and GPC measurements were made on this fluid. The permanent viscosity loss was found to be 56.1%. The results of the GPC tests are shown in Figures 8 through 11. The location of each sample is noted on the corresponding figure. There is virtually no change in the molecular weight distribution (MWD) from the original fluid to the sample taken from the oil reservoir, however there is marked change after the fluid has been sheared. No sample was taken from the entrance region of the EHD contact with this fluid because the original fluid was depleted. The large amount of degradation is more graphically illustrated in Figure 11 which is a composite of Figures 8 and 10. The viscosity loss was calculated from the MW found with the GPC and was found to be 61.4%. The disagreement with the measured viscosity is due to the polydispersity of the unsheared sample which does not correlate well with the viscosity-MW relations.

Fluids S7 and S8 which were specifically blended to

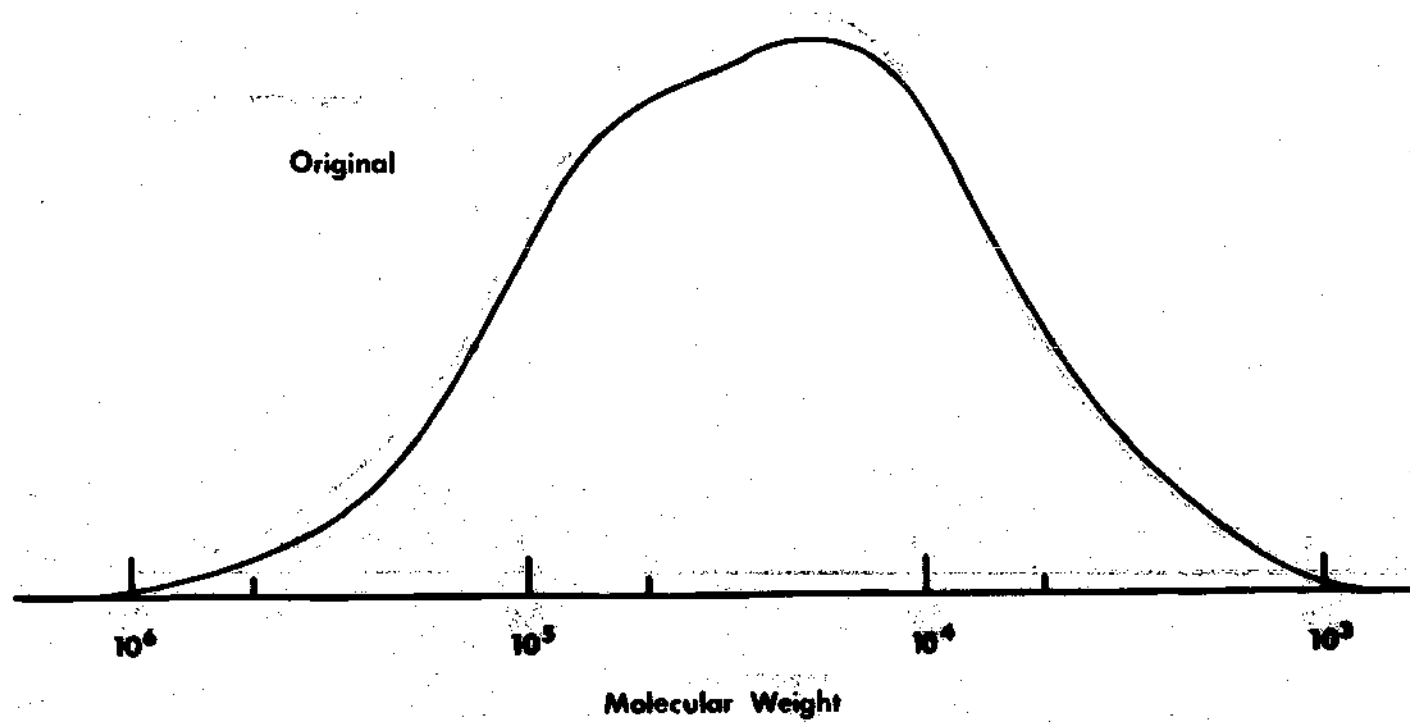


Figure 8 Molecular Weight Distribution, Fluid 56

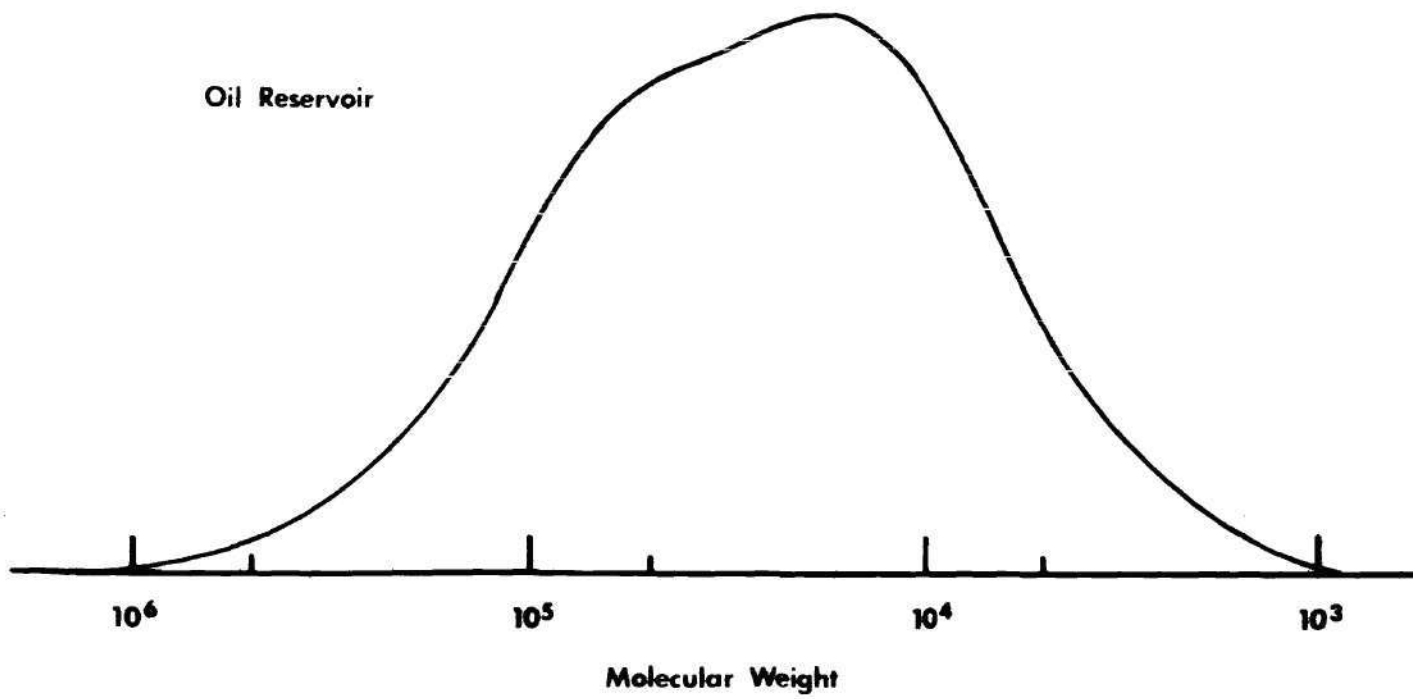


Figure 9 Molecular Weight Distribution, Fluid S 6

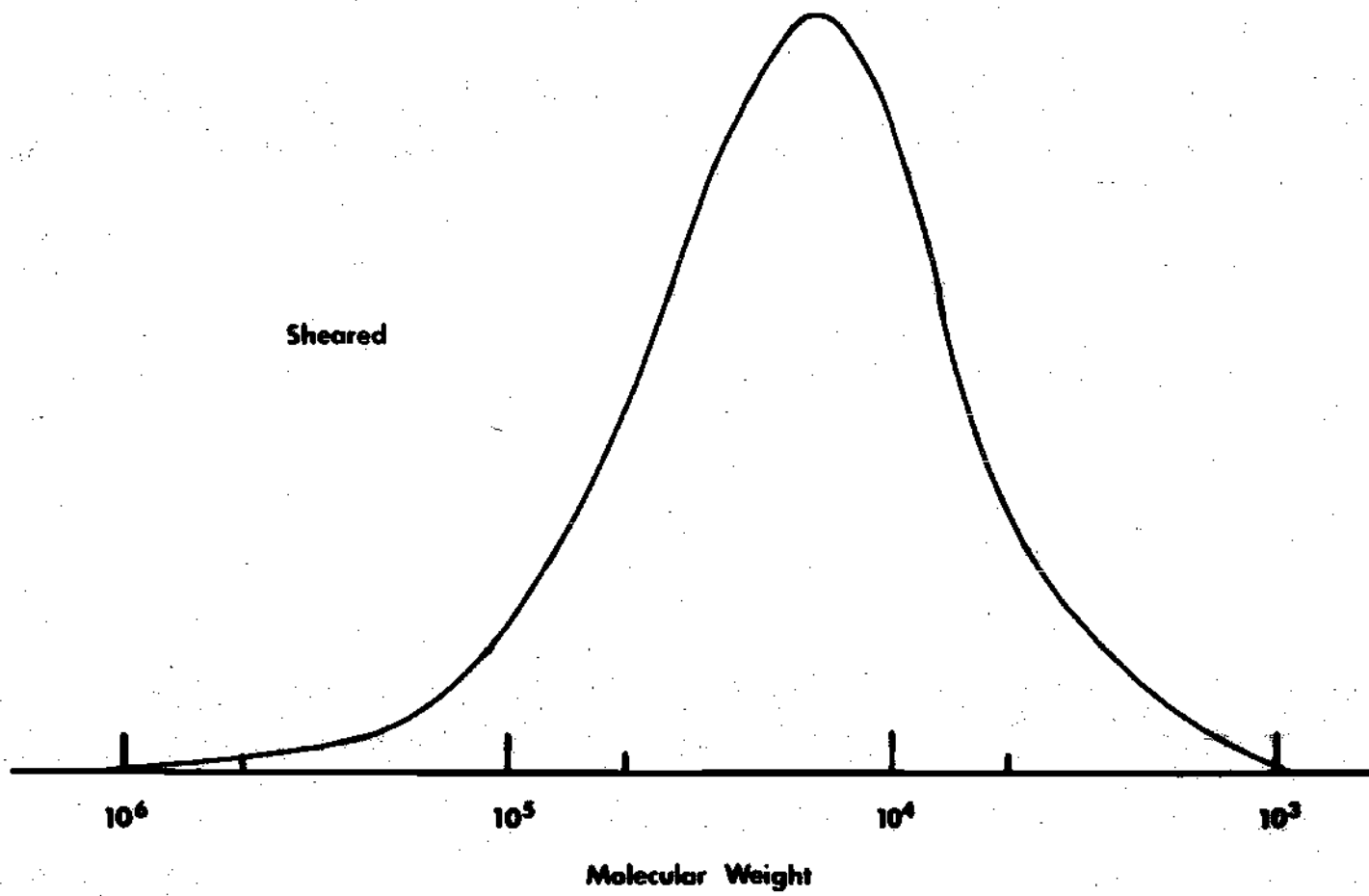


Figure 10 Molecular Weight Distribution, Fluid S.6

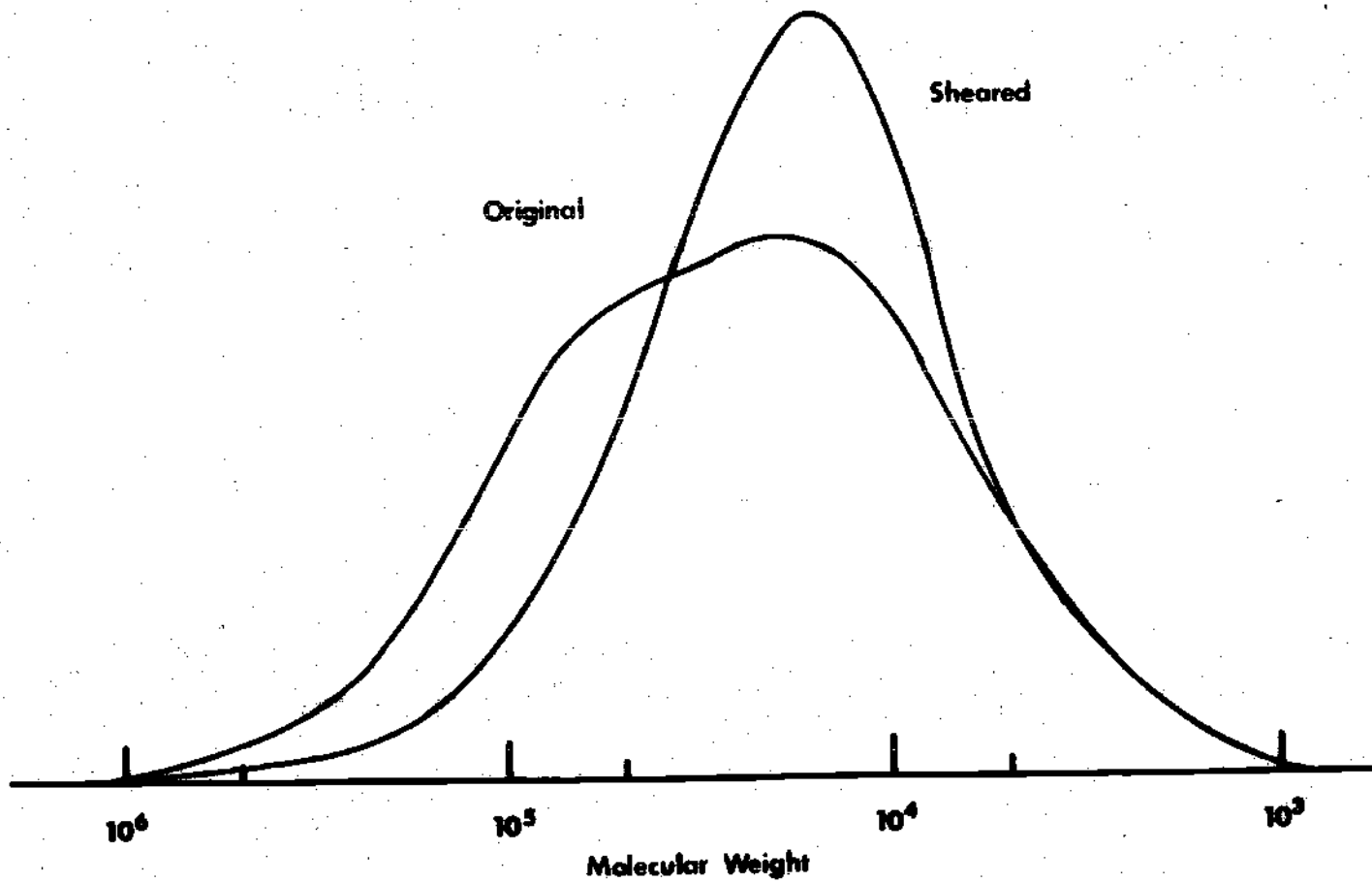


Figure 11 Molecular Weight Distribution, Fluid S6

give an indication of a limiting MW for degradation were not successfully tested. Although a fluid film could be established in the EHD contact for a period of time (less than 30 minutes), the film would collapse before any sample could be taken. This collapse resulted in direct contact between the sapphire and the sphere with subsequent scratching of both in most cases.

Three modes of failure were observed. The most common mode of failure appeared to be a simultaneous scratching of the steel sphere and the sapphire apparently due to starvation caused by small bubbles of air mixed in the fluid. As the fluid was being drawn into the contact the bubbles would also be drawn in. When the bubble entered the contact there was insufficient lubricant to sustain the load and the surfaces made contact. The same result occurs when no lubricant is present. On a few occasions a small piece of foreign matter became lodged in the entrance region and the contact was starved. On one occasion the sapphire scratched and the steel ball remained in good condition. The sapphire was moved by means of the micrometer screws and the apparatus continued to run for a short period of time (10 minutes) before both sphere and sapphire scratched. Figures 12 and 13 show the MWDs for these two fluids and by comparison with the unsheared samples of fluid S6, it can be seen that there are two differences between these silicones. Fluids S7 and S8 have a greater concentration of high MW fractions and are

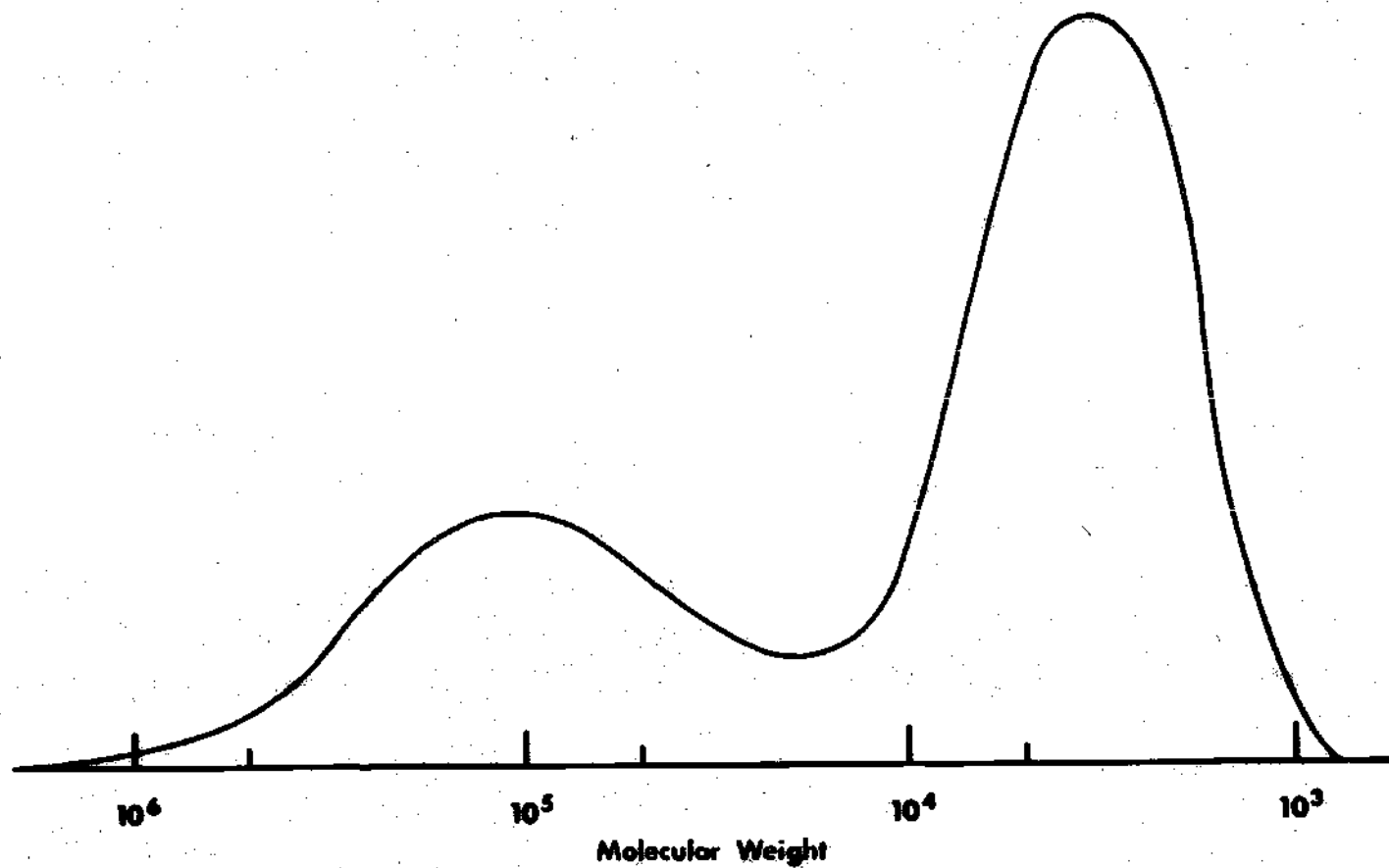


Figure 12 Molecular Weight Distribution, Fluid S7

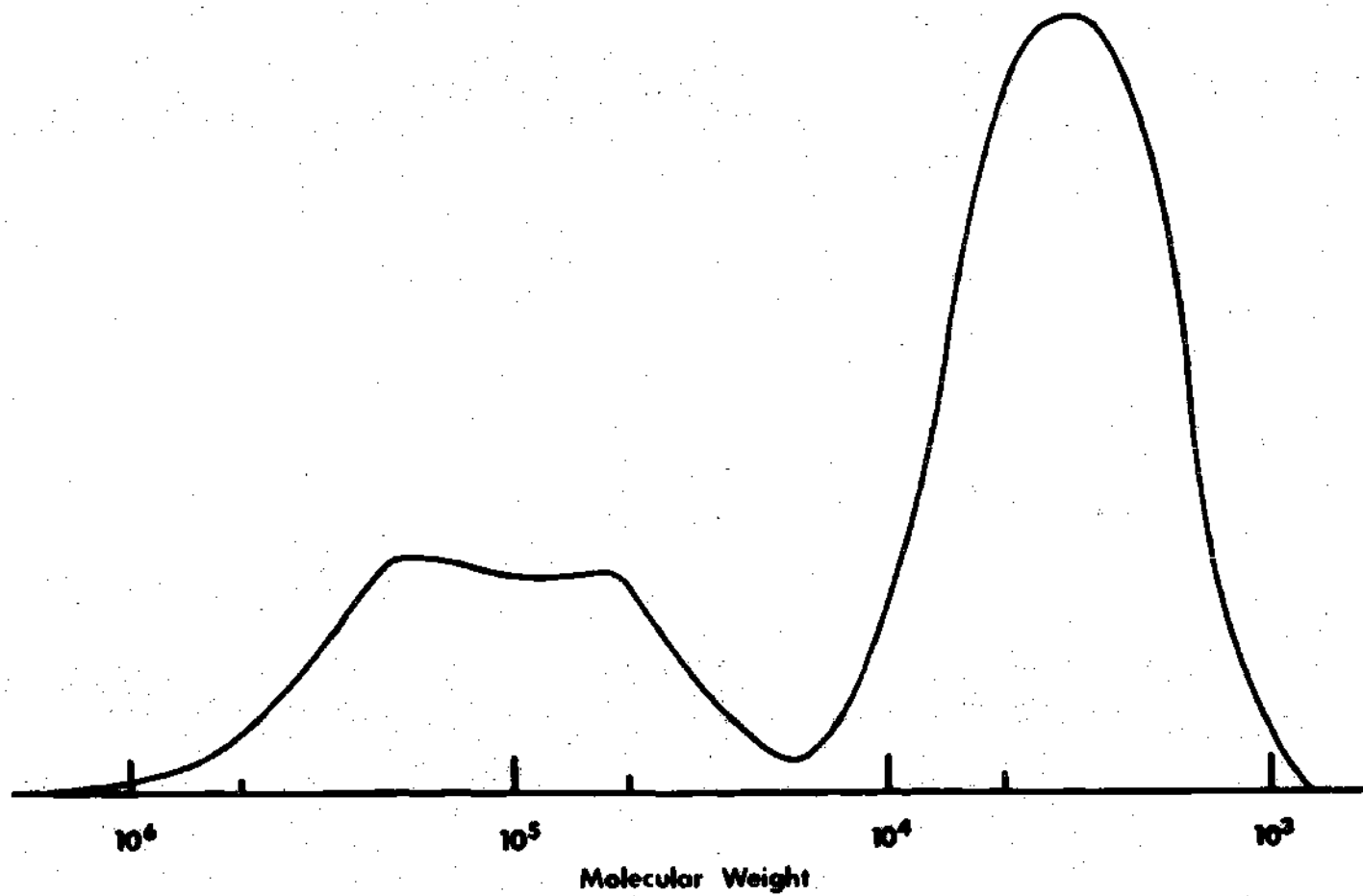


Figure 13 Molecular Weight Distribution, Fluid 58

more disperse in makeup. How these differences might explain the greatly different behavior of these fluids is unknown. How the sapphire could scratch without marring the sphere is also unexplained.

Other Synthetics

A very slight increase in viscosity and MW (as determined from GC made by Monsanto, the lubricant manufacturer) was found in the sheared samples of fluid S9; however, these changes were both within experimental error. A very small amount of a very low boiling point substance was found in all of the samples except the original fluid. It is thought that these might be some indication of degradation; however it may be concluded to be insignificant.

Fluid S1 exhibited a marked increase in viscosity, 4.3%; however, no chemical test utilized could detect any change in composition of the fluid. The tests tried were IR spectroscopy, GC, and mass spectroscopy. It was later determined that none of these techniques could accurately determine a small shift in the relative composition of the test samples.

The increase in viscosity is typical of what has been found in extended service conditions [27] and is due to a shearing off of a hexyl end group leaving a "free" oxygen. This oxygen forms "hydrogen bonds"; i.e., electrostatic bonds, with hydrogen atoms of adjacent molecules, forming a polymer that has the same effect as a crosslinking of

molecules but does not significantly change the composition of the fluid. Degradation of this kind of less than 0.5% can cause the viscosity increases that were measured [27]. For this fluid, determination of the number of "free" oxygens by dye chemistry would be a better method of finding degradation.

Organic Hydrocarbons

The paraffinic base oil, P1, was tested in the Haake Rotovisco and a small decrease in viscosity was found, 1.6%; however, this is within the experimental error ($\pm 2\%$) of this particular apparatus. No further tests have been done on this sample as of this date because no adequate equipment is available.

The permanent viscosity decrease in the PAMA solutions, fluids P2, P3, and P6, was found to be extreme, up to 70%. In fact all of these mixtures were reduced in viscosity to the region of the base oil, P1. The GPC-MWD curves for the polymer additives are shown in Figures 14 through 28. These chromatographs were made by Rohm and Haas Company, manufacturers of the PAMA additives. Each stage of testing is shown in order for each fluid and a composite of the original distribution, as supplied by the manufacturer, and the sheared distribution is also shown. It can be seen that only a small amount of shearing takes place in the oil reservoir and the entrance region of the EHD contact. The composite figures emphasize the large degree of degradation

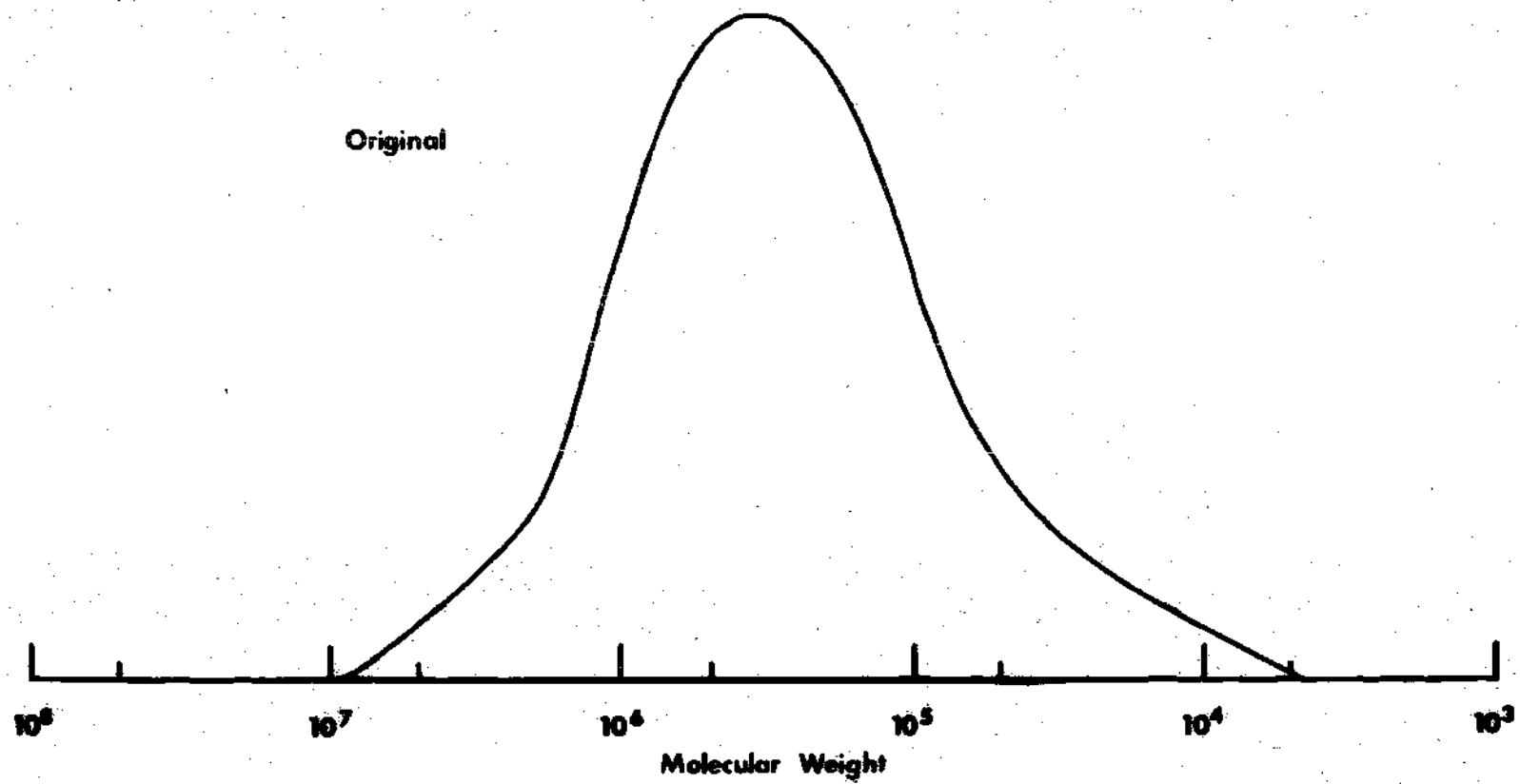


Figure 14 Molecular Weight Distribution, Fluid P2

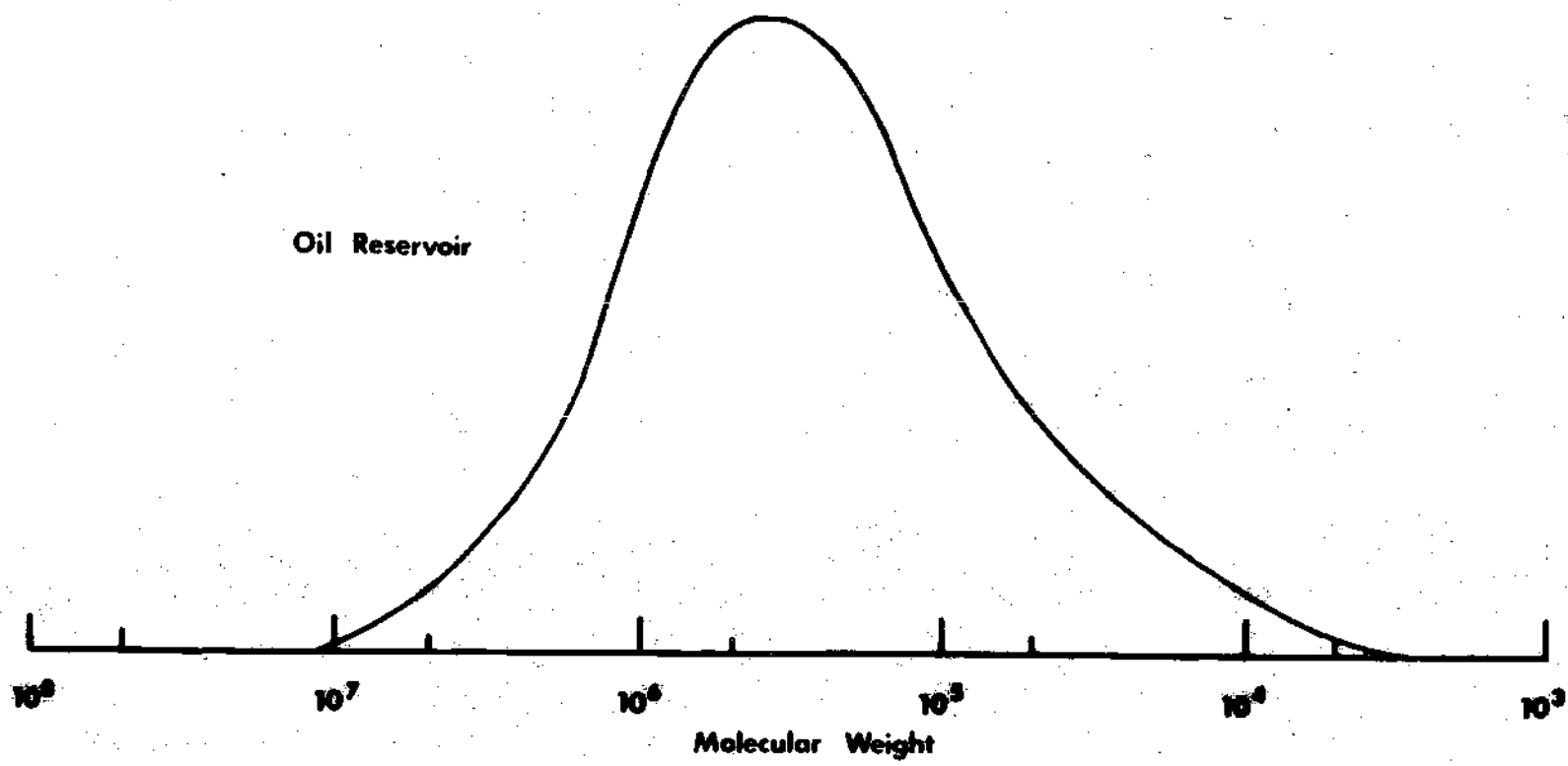


Figure 15 Molecular Weight Distribution, Fluid P2

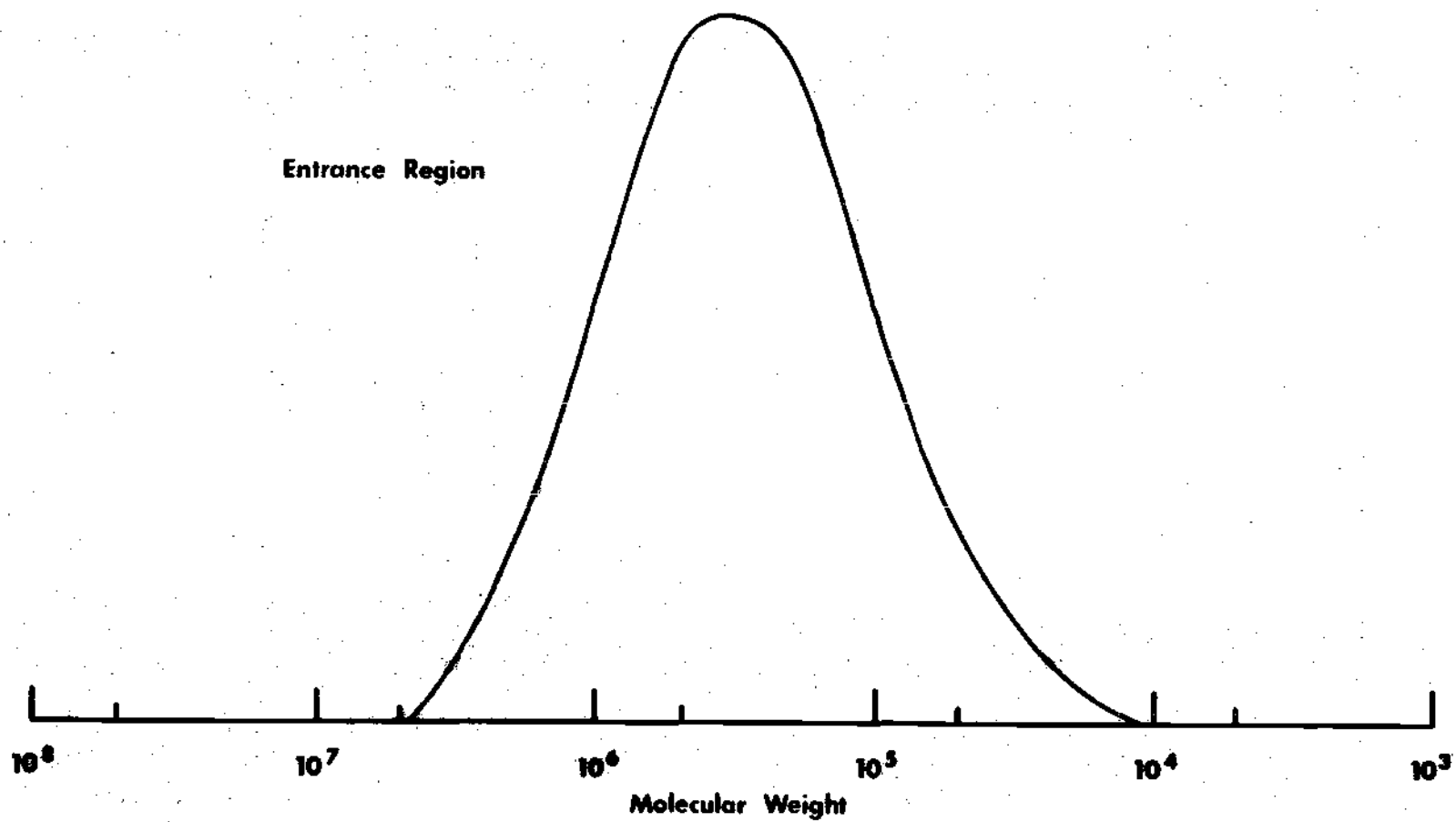


Figure 16 Molecular Weight Distribution, Fluid P2

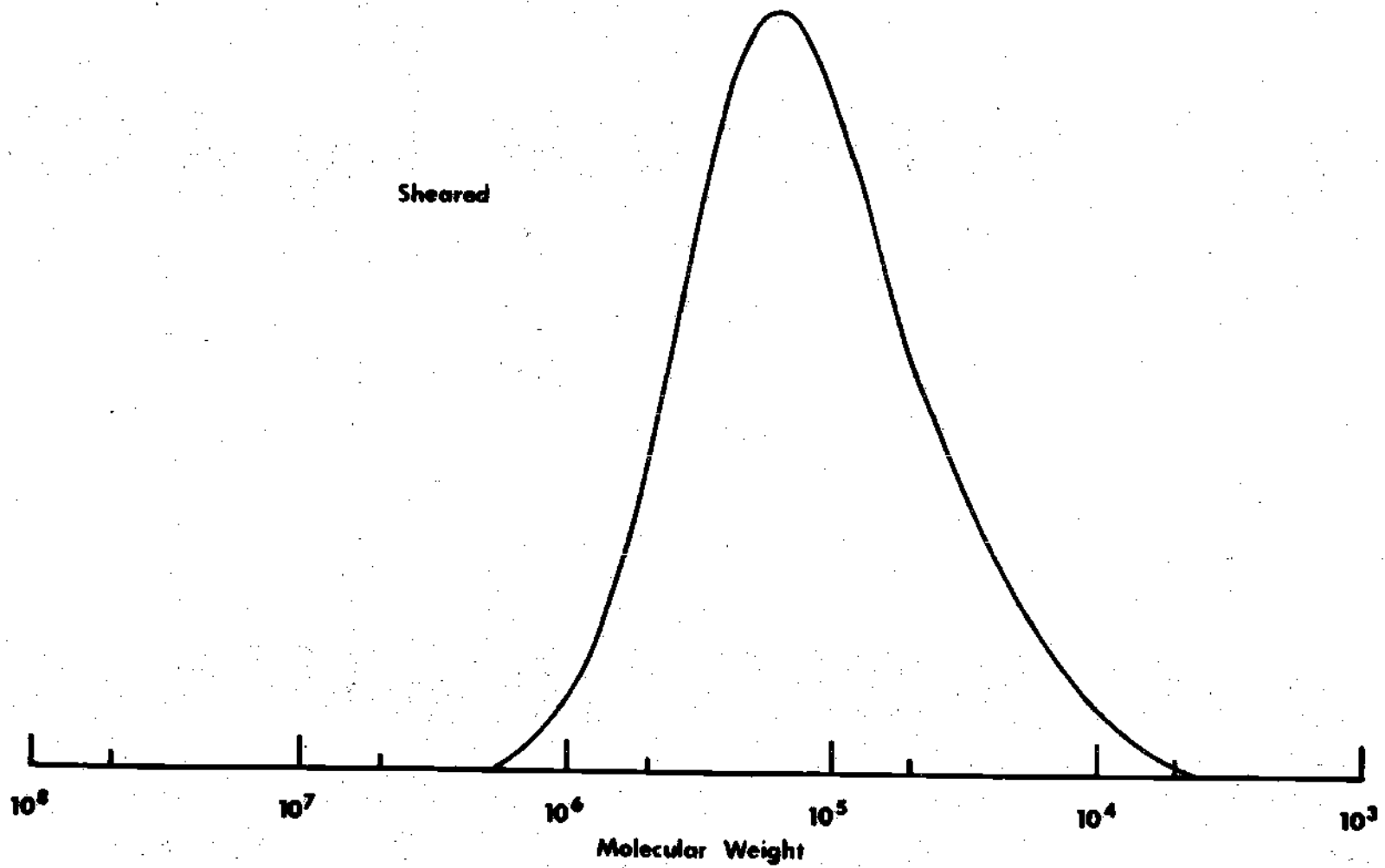


Figure 17 Molecular Weight Distribution, Fluid P2

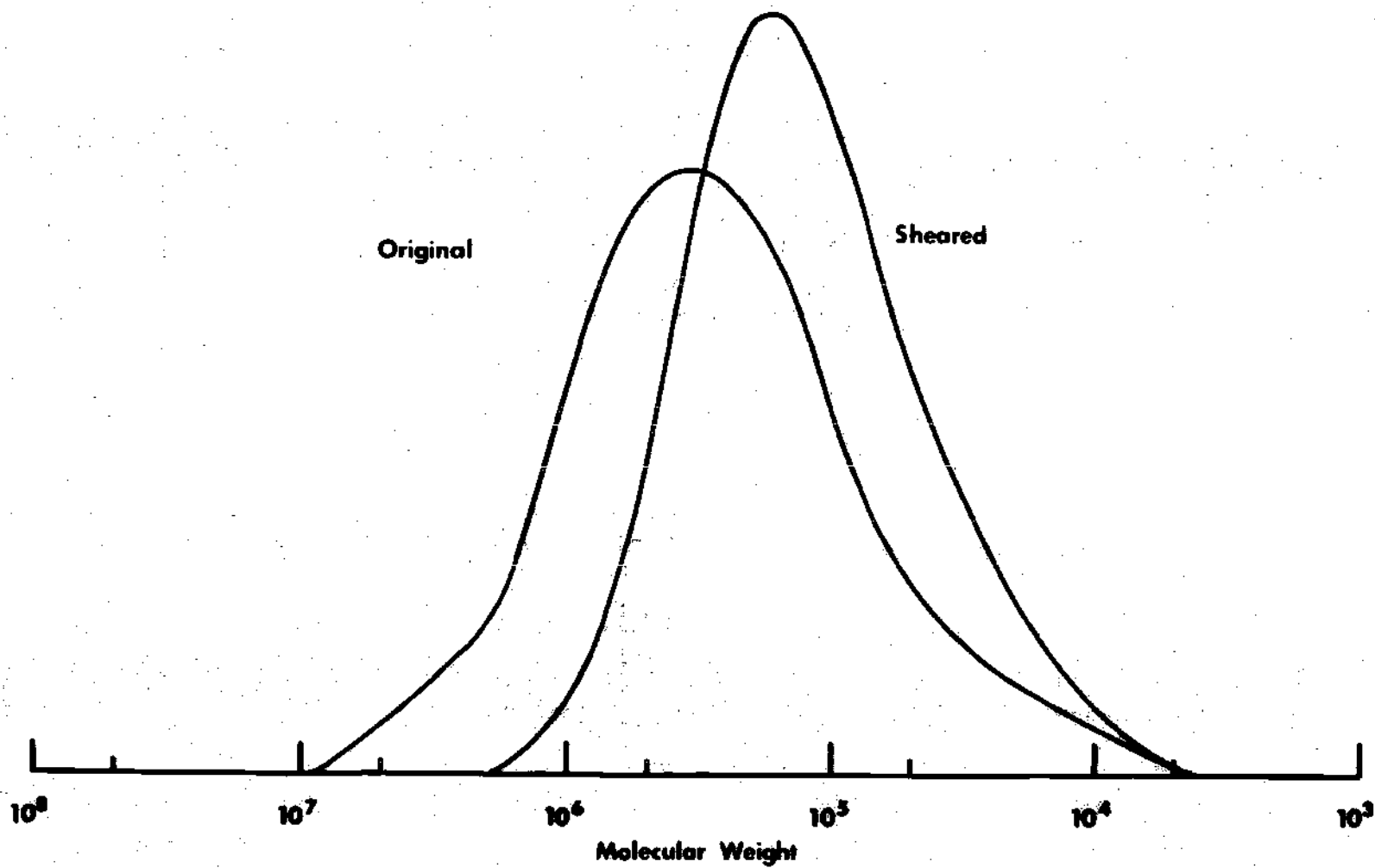


Figure 18 Molecular Weight Distribution, Fluid P2

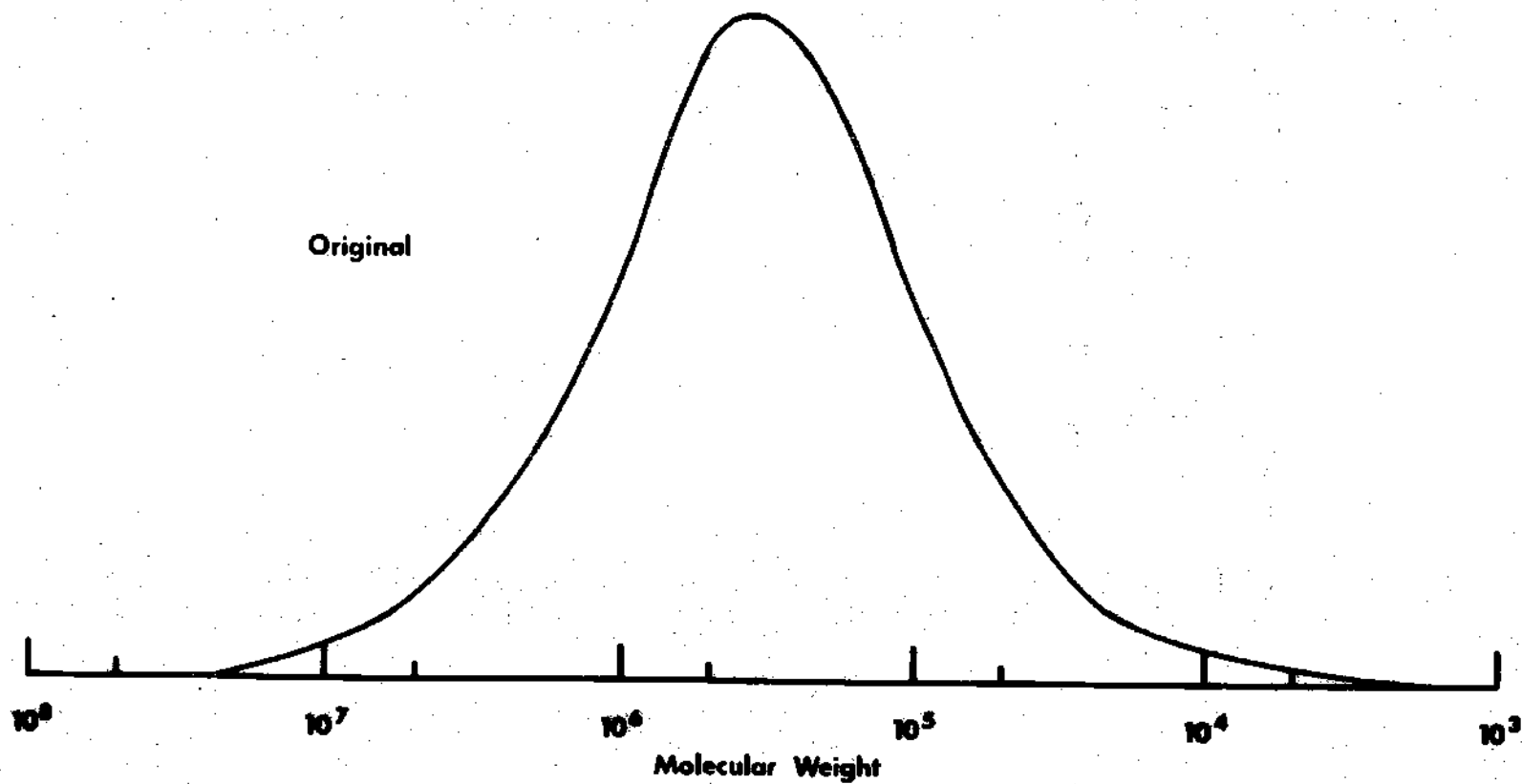


Figure 19 Molecular Weight Distribution, Fluid P3

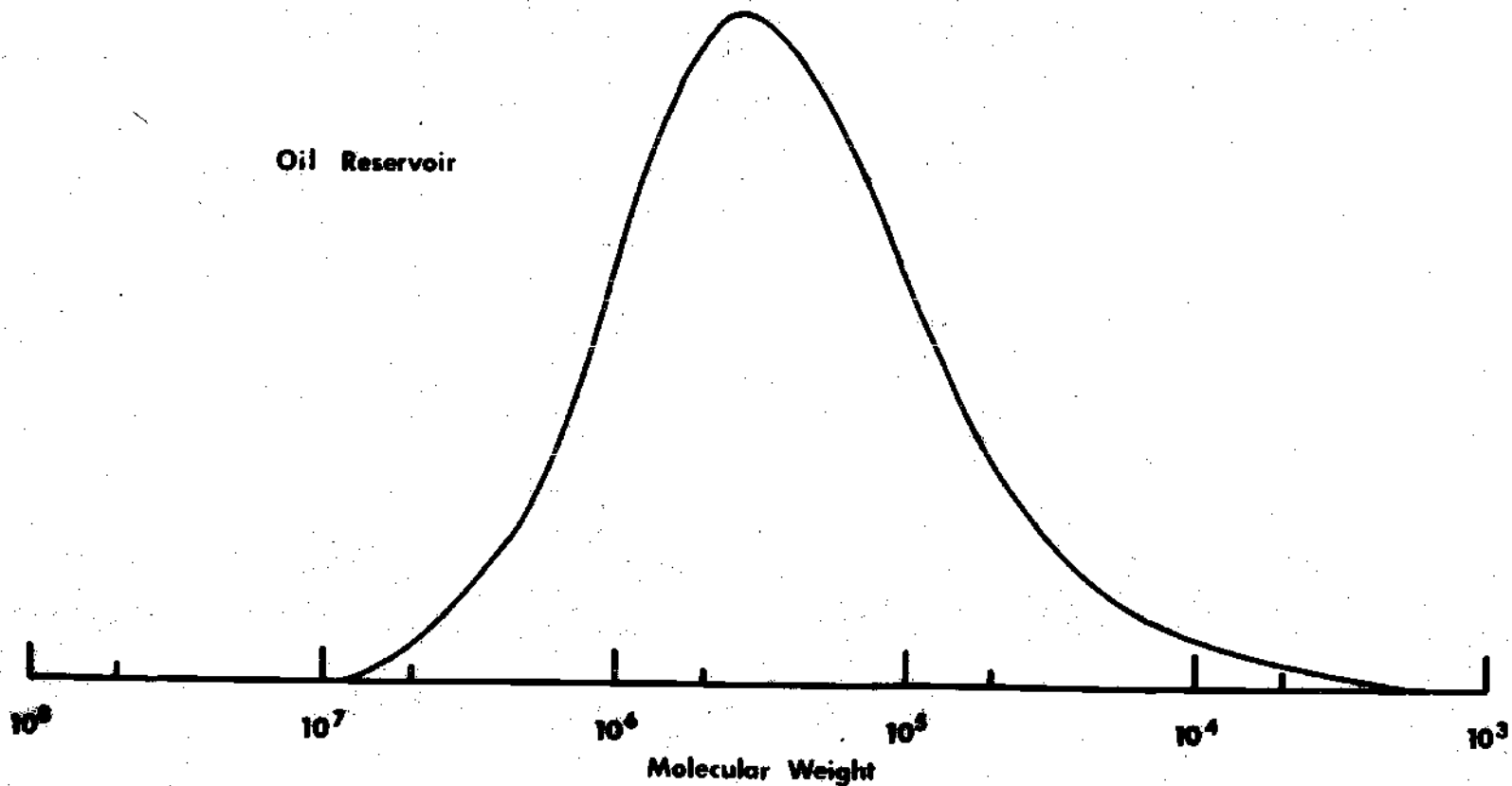


Figure 20 Molecular Weight Distribution, Fluid P3

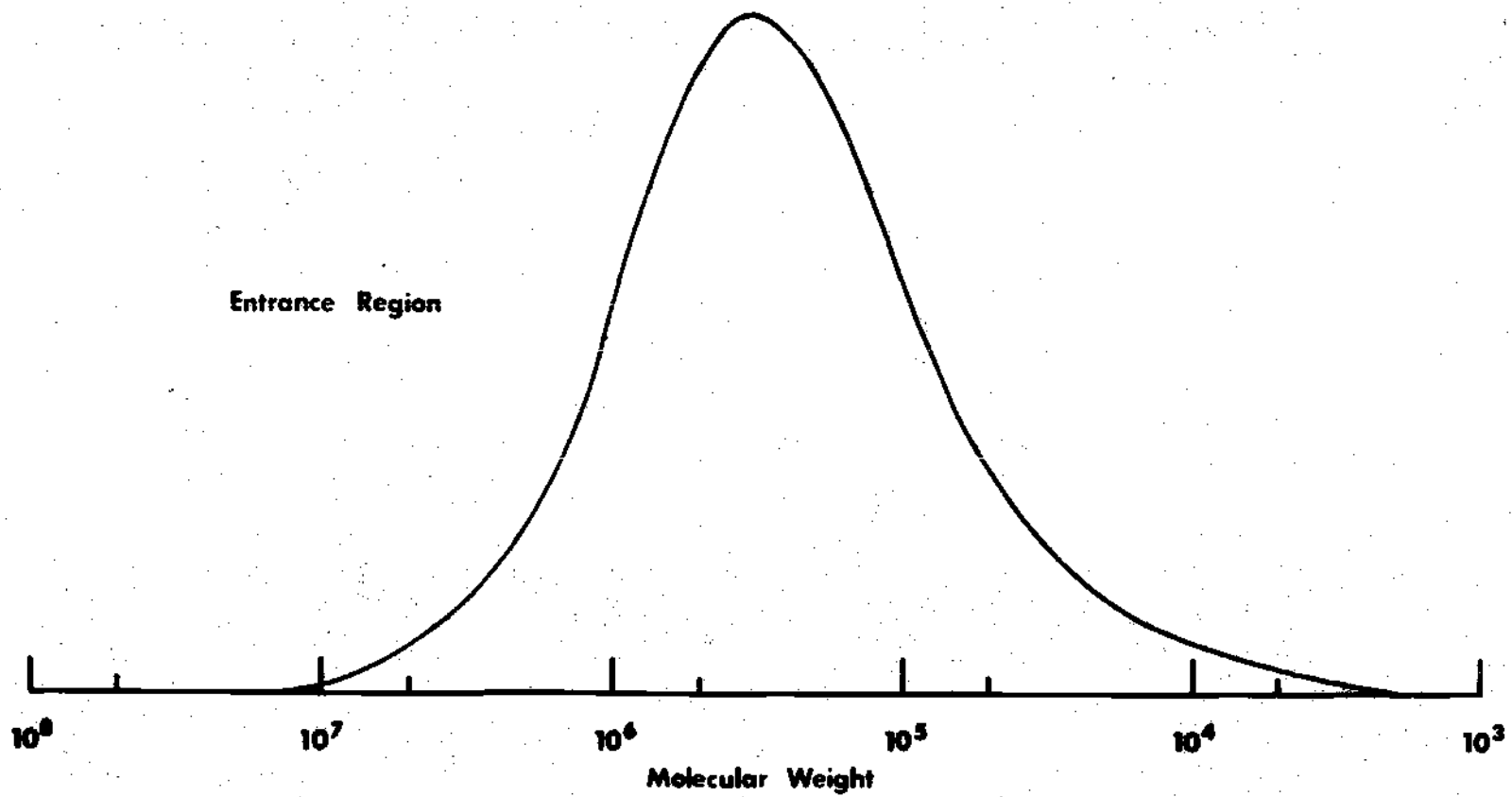


Figure 21 Molecular Weight Distribution, Fluid P3

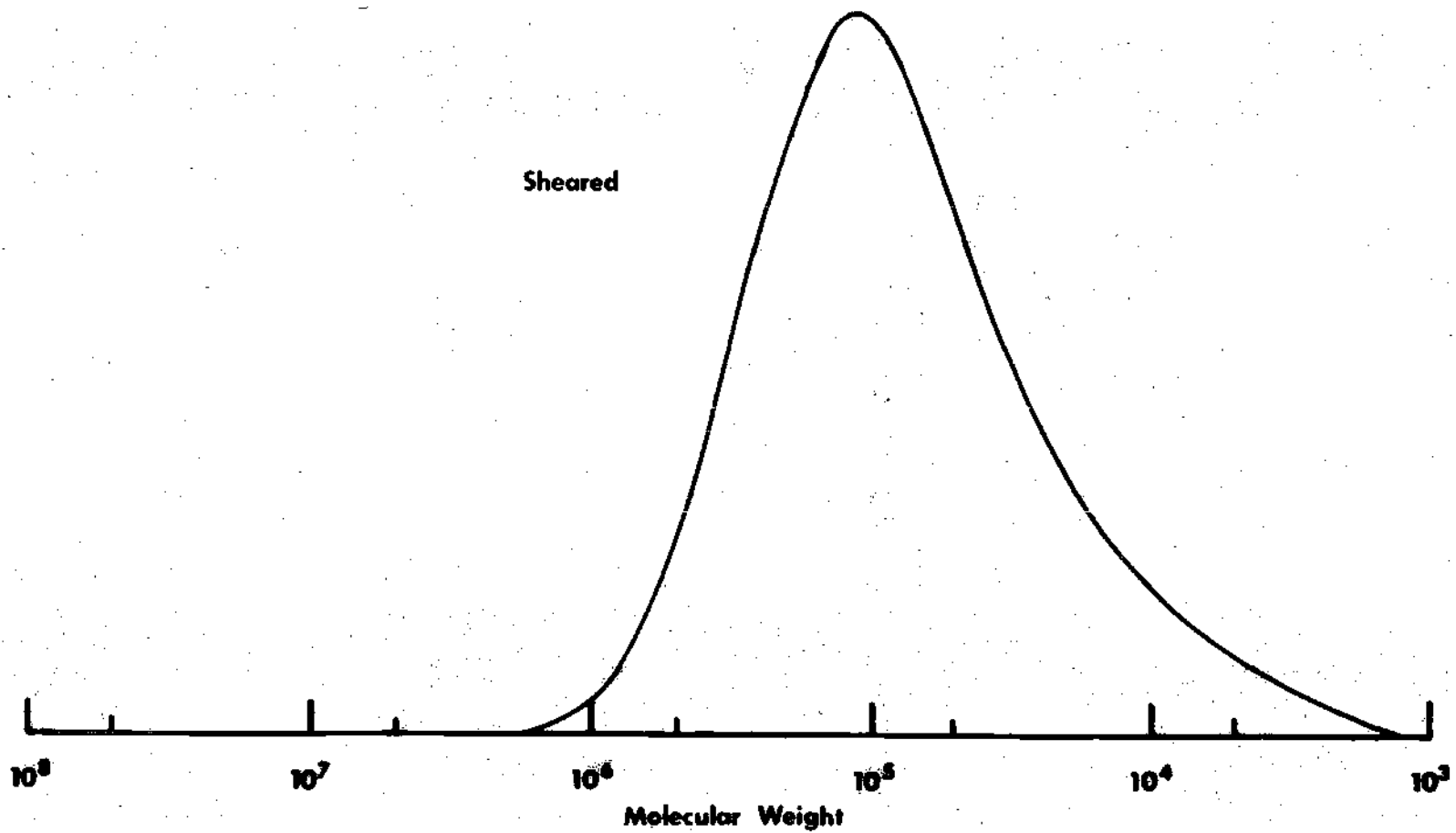


Figure 22 Molecular Weight Distribution, Fluid P3

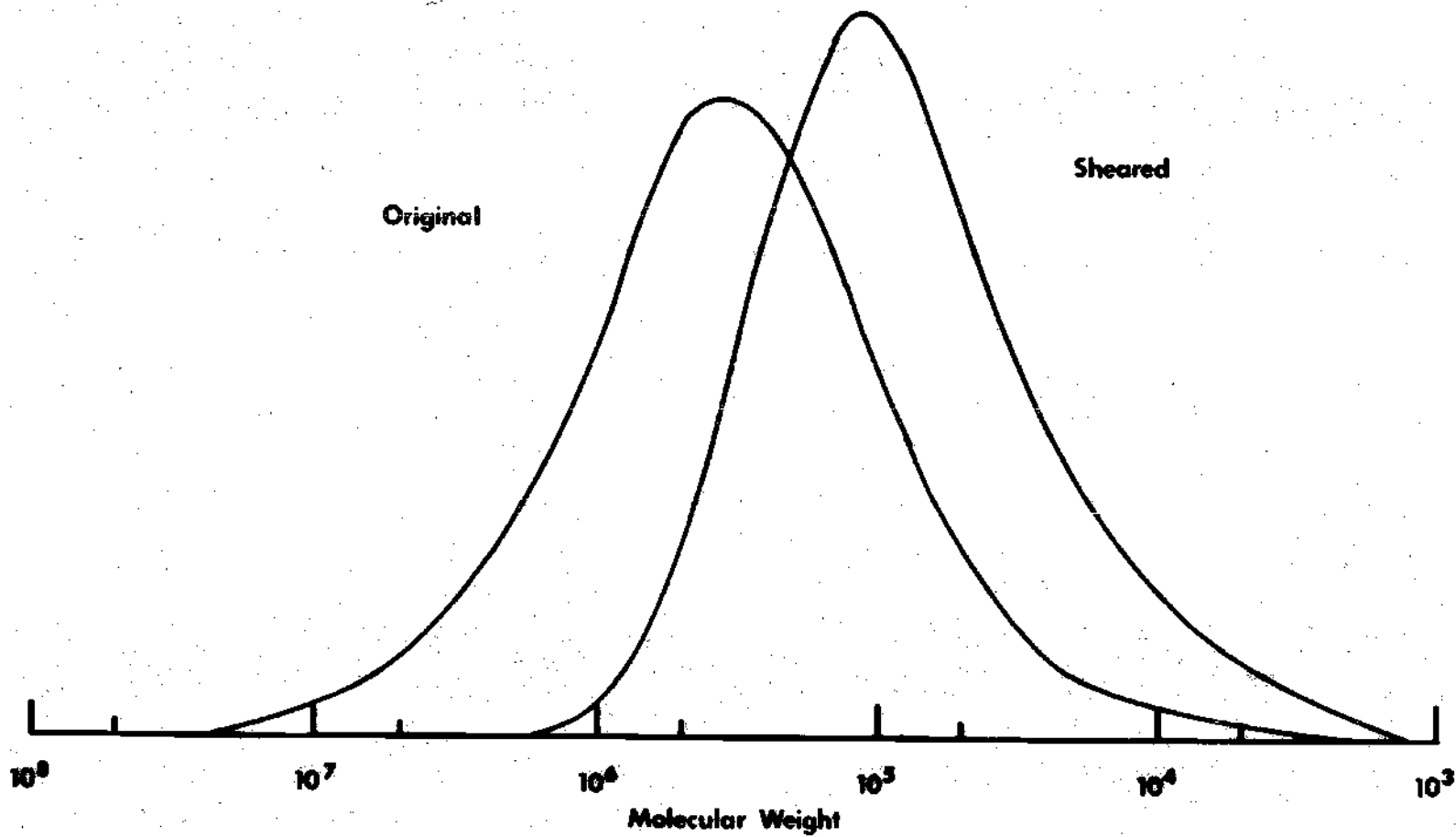


Figure 23 Molecular Weight Distribution, Fluid P3

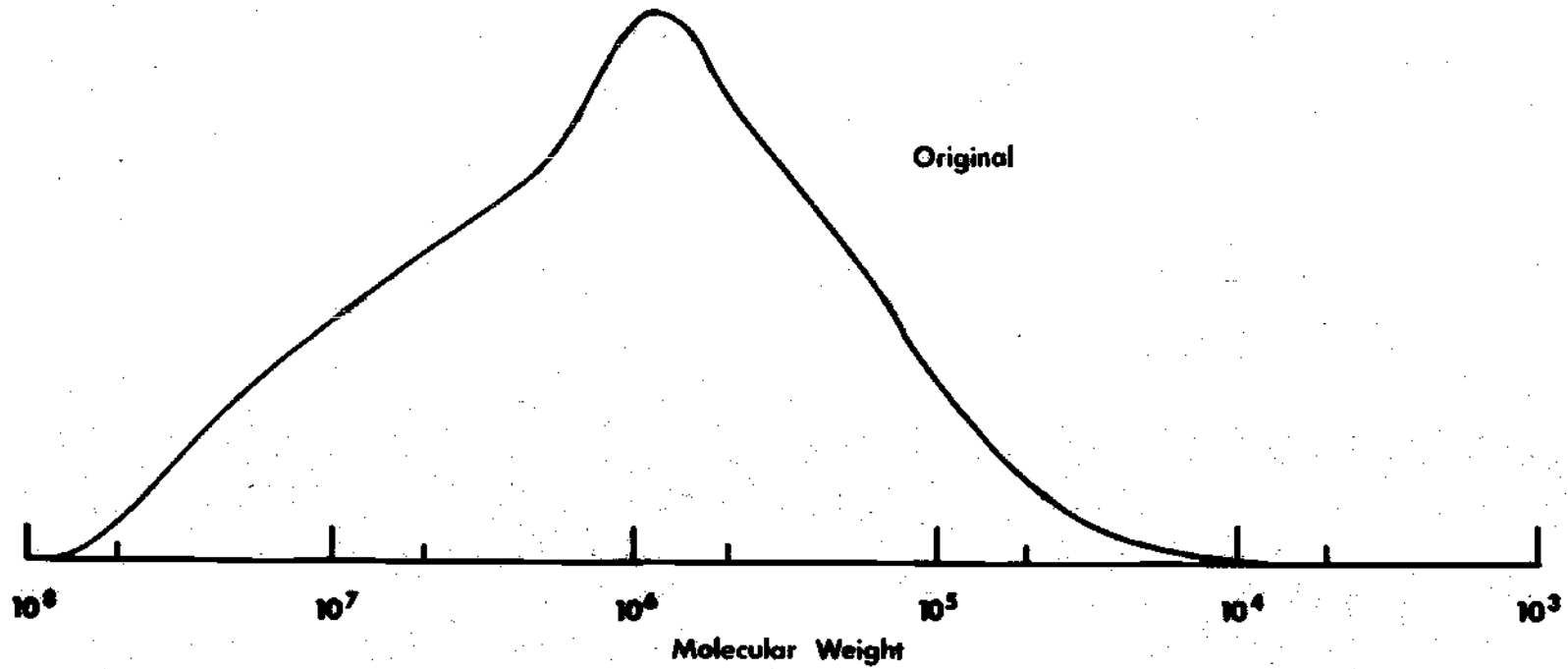


Figure 24 Molecular Weight Distribution, Fluid P6

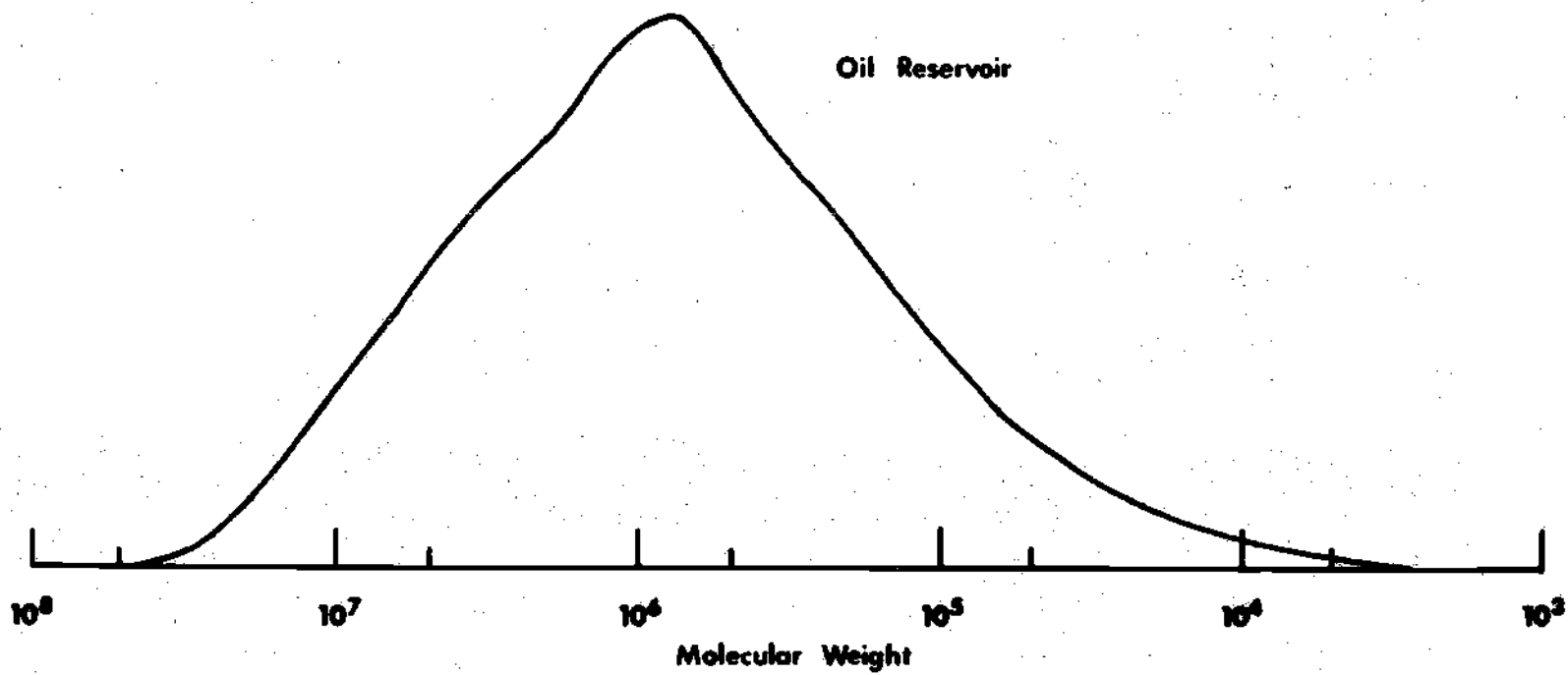


Figure 25 Molecular Weight Distribution, Fluid P6

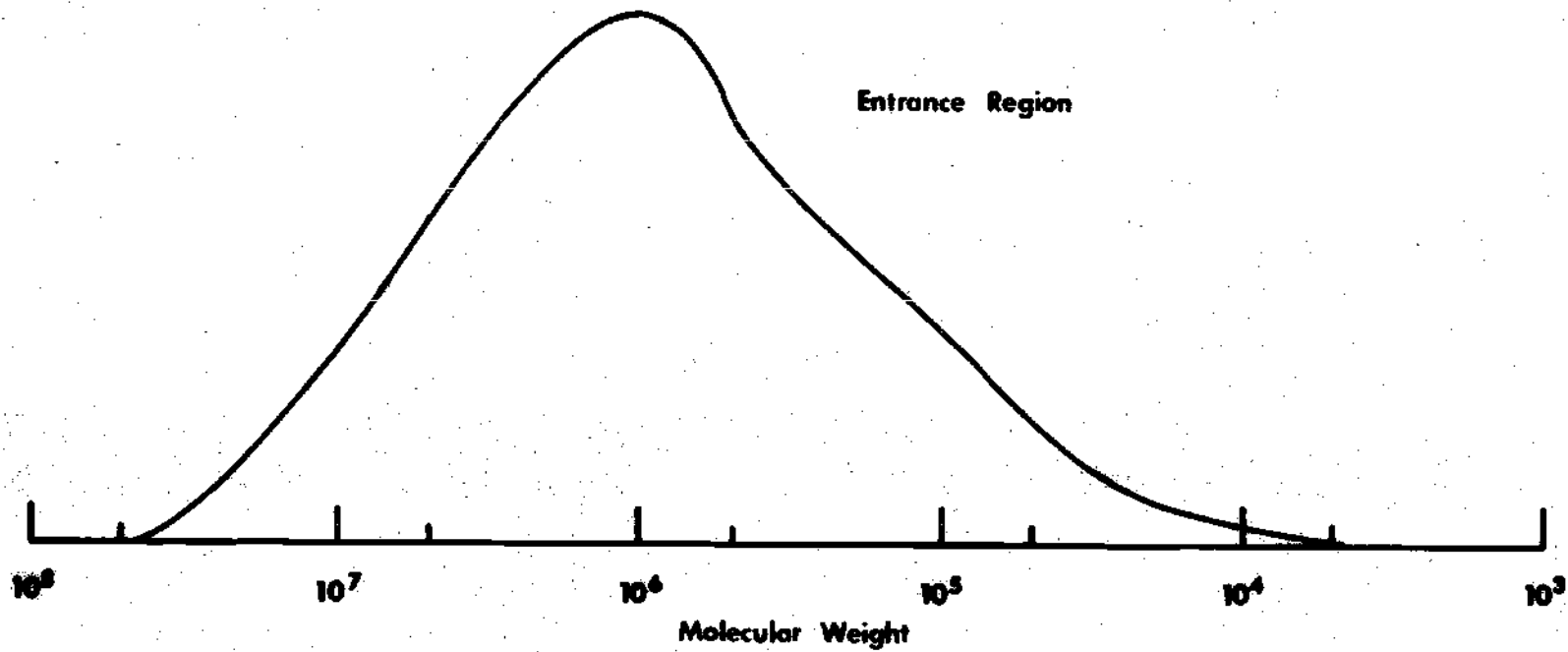


Figure 26 Molecular Weight Distribution, Fluid P6

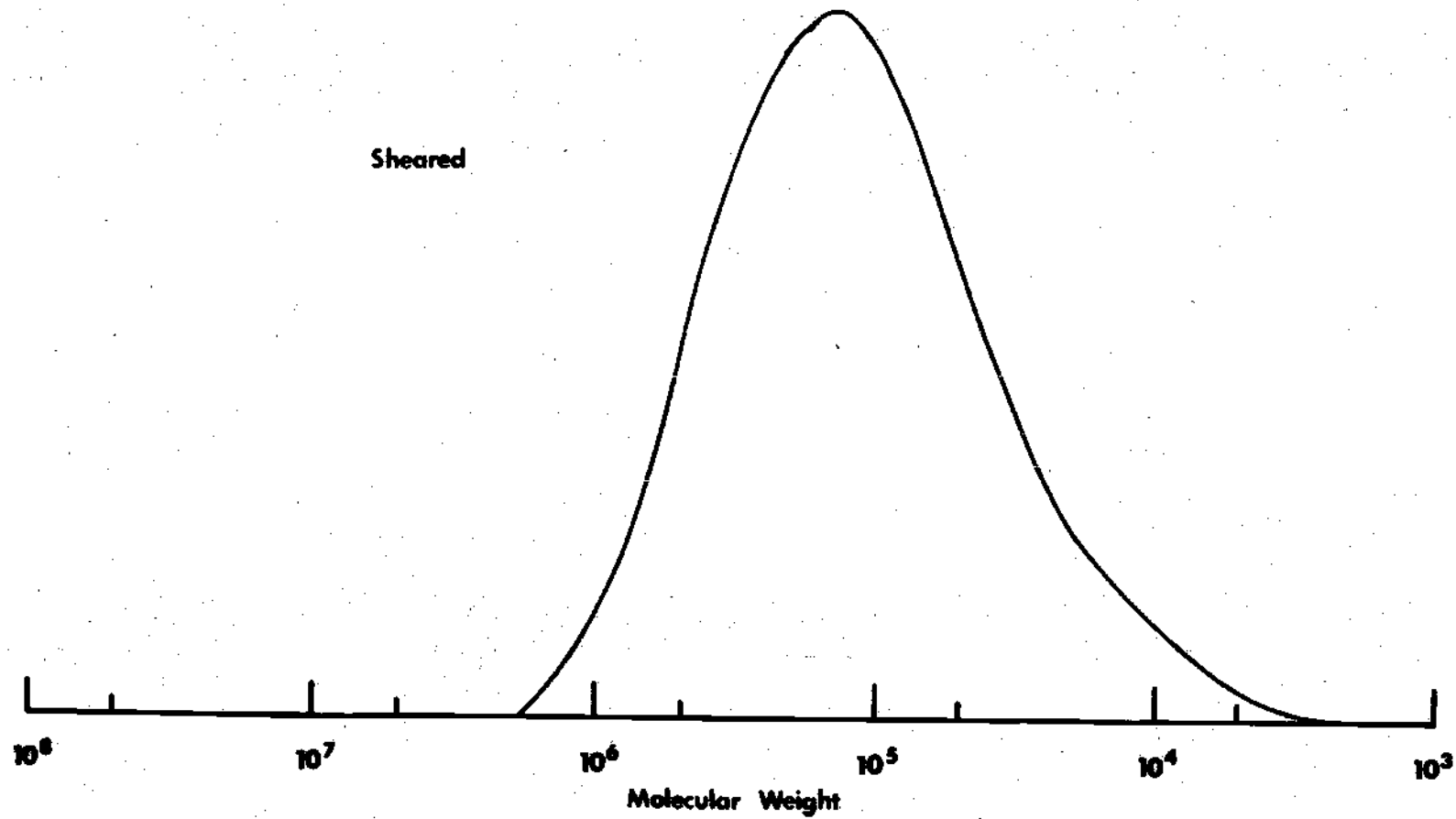


Figure 27 Molecular Weight Distribution, Fluid P6

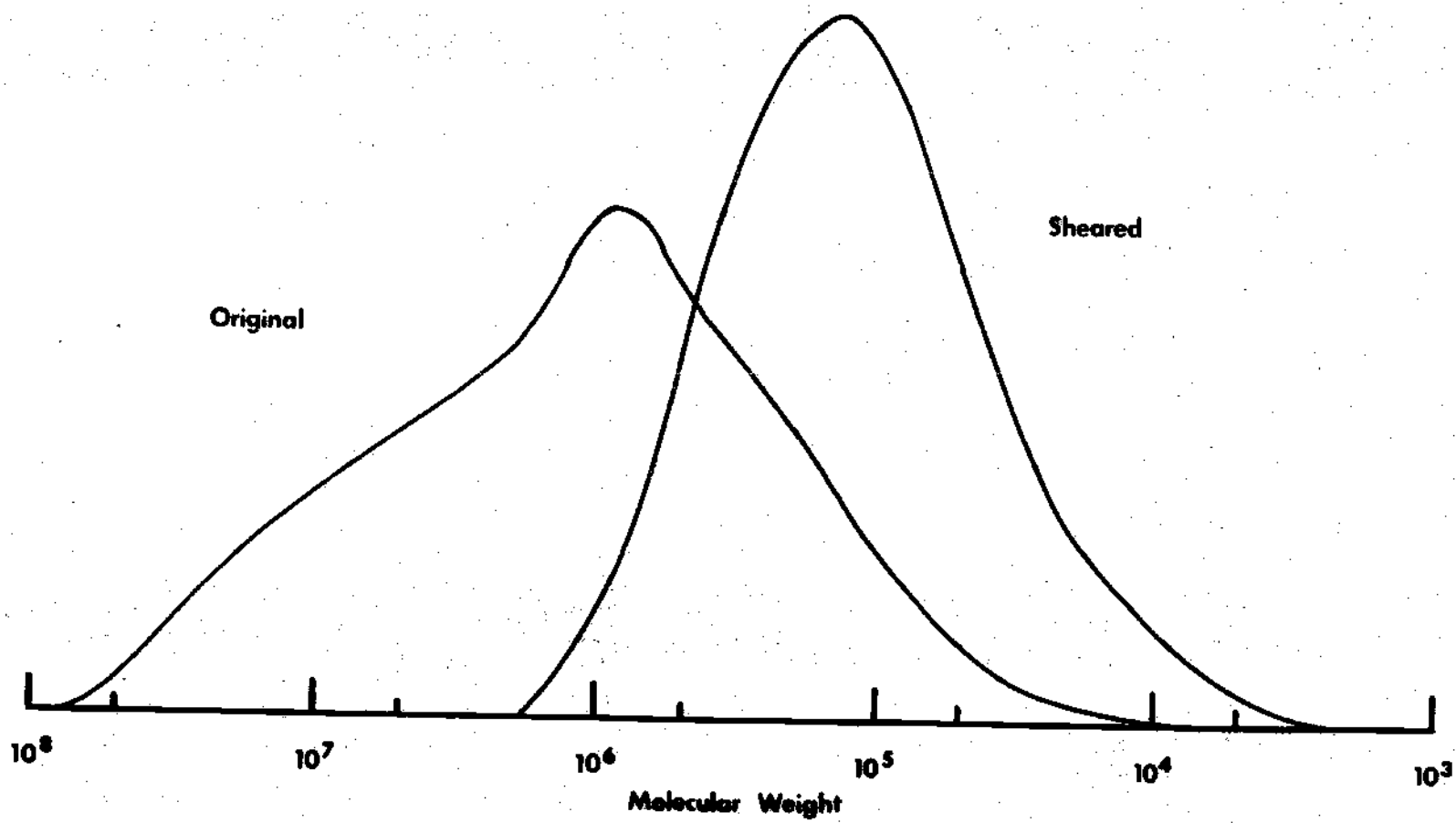


Figure 28 Molecular Weight Distribution, Fluid P6

that takes place in the contact. In every case the distributions are being reduced to a closer approximation of a Gaussian distribution and it is probable that further shearing will not greatly change the shape of the curves but will shift them to a lower point on the MW scale. The MWs that are calculated from this data and shown in Table 4 cannot be taken as exact numbers due to the difficulty of working with the very high MW fractions that are present in these fluids. However the percentage change in MW as calculated from the viscosity and from the GPC data agrees very closely.

General

In order to determine if there is a general correlation between energy input into the fluid, ϵ , and permanent viscosity loss or degradation, these quantities were plotted in Figure 29. The abscissa of this plot is the energy input into the fluid. The ordinate is the ratio of the original and final viscosities or the corresponding MWs as shown. In the case of the polymer solutions all of the energy dissipated was assumed to go into the polymers and none into the base oil. The relatively minor change found in the base oil justifies this assumption. It can be seen that the MW ratio correlates in a general way with ϵ , and is better than was expected for such different fluids. The viscosity ratio also correlates generally; however, the bulk silicone polymer no longer fits as well. Many more data points are needed

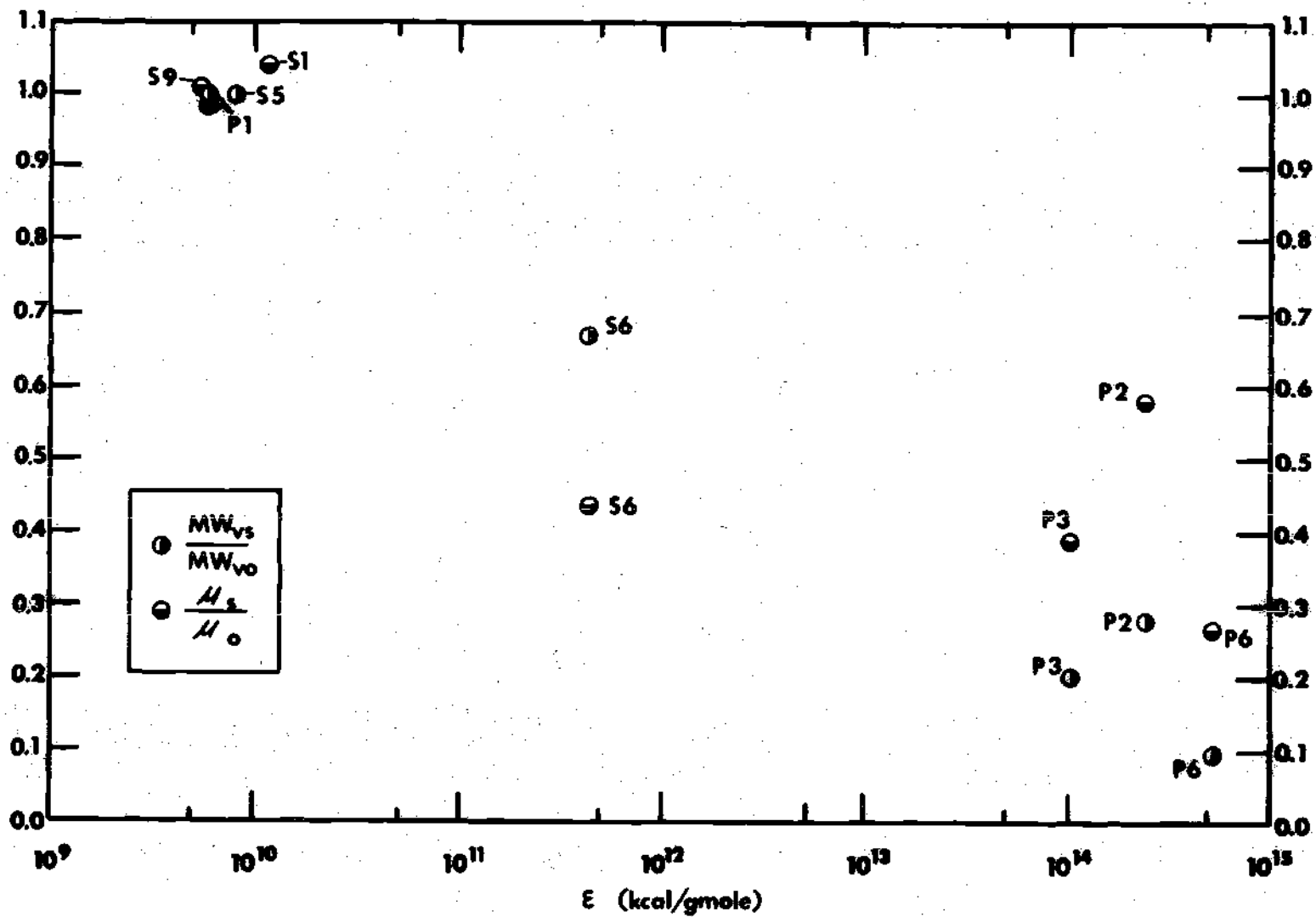


Figure 29 Energy Input Versus Molecular Degradation and Viscosity Loss

before any concrete conclusions can be reached. Figure 30 is a similar plot where the energy input rate per unit volume, E , is the abscissa. It can be seen that there is no correlation using this scale.

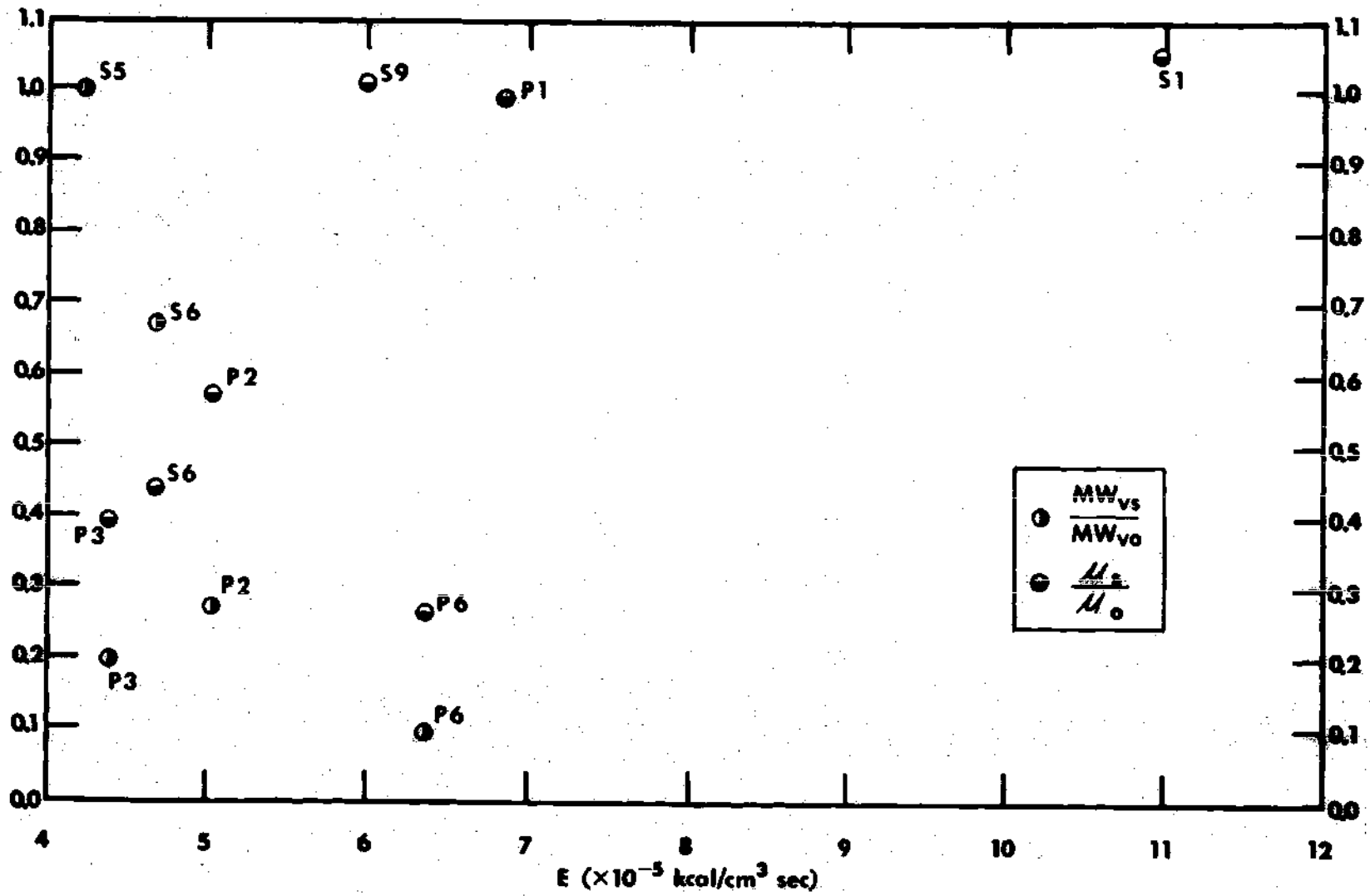


Figure 30 Energy Input per Unit Volume Versus Molecular Degradation and Viscosity Loss

CHAPTER VI

DISCUSSION OF RESULTS

In this investigation a new technique was developed which allows the sampling of oil which has passed through an EHD contact. This method makes possible the examination of undiluted samples of highly sheared oil. These samples of oil were then investigated using various analytical techniques in order to determine permanent changes in the fluids. The viscosity and the molecular weight distribution were investigated to determine if the fluid had been modified by shearing in the EHD contact.

A variety of fluids were examined. These included bulk polymer lubricants, hydrocarbon lubricants, and polymer containing hydrocarbon solutions. A significant change in viscosity was found in five of the ten lubricants tested, with a maximum decrease of seventy percent. For the remaining five lubricants, three were not significantly changed, and two were not successfully tested. Changes in molecular weight were found with a maximum decrease of ninety percent. This large amount of polymer degradation indicates that this may be the primary source of polymer degradation which has been found in earlier studies which used automotive engines as test apparatus. The permanent viscosity loss also

appears to explain the disagreement that has been previously reported between experimental data and theoretical predictions of film thickness for these high polymer fluids.

The behavior of certain fluids under high shear conditions has previously been given as the reason for the lack of agreement between theory and experiment in EHD lubrication. For the hydrocarbon solutions tested in this study, this lack of agreement can be explained by permanent degradation of the fluid. In a previous publication, Sanborn and Winer [12] determined an apparent viscosity loss, S , by estimating an effective viscosity, μ_e , which would bring their film thickness data for high MW fluids into agreement with data for Newtonian fluids. This apparent viscosity is calculated by the equation

$$S = 1 - \frac{\mu_e}{\mu_0}$$

By substituting the sheared fluid viscosity, μ_s , as measured in this study, for the effective viscosity, a comparable permanent viscosity loss, S_p , can be determined. Table 5 lists these values for the fluids which were studied in both works. The correlation is apparent, the qualitative differences are partially explained by the fact that the base viscosities were measured at different temperatures; In Sanborn's work, μ_0 was measured at room temperature, while measurements for this study were taken under conditions

Table 5. Apparent and Permanent Viscosity Loss

Fluid	S	S _p
P1	0.00	0.02
P2	0.26	0.42
P3	0.54	0.61
P6	0.63	0.74
S1	0.00	-0.04

previously explained. The samples examined in this study were taken from the center of the contact and have the longest residence time in the contact. The film thickness is determined by the fluid at the entrance region of the contact and the entire area of contact.

A general type of correlation between energy input to the fluid and viscosity or molecular degradation was found. It is possible that with proper development this can be useful as a guide in formulating lubricants. For the present, the machine designer must assume that only the base oil viscosity is applicable to EHD lubrication conditions. With bulk polymers each fluid must be tested for each application. This is illustrated by the results with the silicone fluids. Three silicones with similar viscosities were tested in the apparatus. One fluid showed a large amount of degradation but was adequate as a lubricant. The other two silicones which had larger fractions of high molecular weight polymers were not good lubricants and could not be tested under EHD conditions. It is thought that molecular degradation can possibly be predicted with a correlation to energy input, but this will be useless for bulk polymer fluids containing high molecular weight fractions until this type of failure is explained. The failures occurred after the tests had been in progress for a short period of time (less than 30 minutes). This behavior suggests some form of progressive mechanism and it is possible that heating may be involved.

CHAPTER VII

CONCLUSIONS

In this investigation a new technique was developed that allows the sampling of a lubricant directly from an EHD contact. In the EHD contact the fluids are subjected to a maximum pressure of 150,000 psi and shear rates up to 2×10^7 sec^{-1} . Hydrocarbon fluids, synthetic bulk polymers, and polymer containing hydrocarbon solutions were tested. The samples of lubricant which had passed through these conditions were tested to determine if they had been modified. The viscosities of the fluids were measured and their molecular weight distributions were determined.

The fluids with low molecular weights (less than 1000) were not significantly degraded, although the viscosity of one fluid, the diester fluid S1, was changed. All fluids of larger molecular weight were significantly degraded and the corresponding viscosities altered.

The viscosities of the polymer containing hydrocarbon solutions were reduced to the region of the base oil. This permanent viscosity loss is the reason for theoretically predicted film thicknesses not agreeing with experimental data. When designing machine elements for use with this type oil, the safe design is to assume that only the base

oil is present for EHD conditions. For bulk polymer lubricants with high molecular weight fractions, each design must be tested with a given lubricant.

General trends were established which indicate that correlations may exist between energy input into the fluid and permanent viscosity loss or molecular degradation. With proper development, these can be useful in the selection of fluids for given applications or in the design of lubricants.

CHAPTER VIII

RECOMMENDATIONS

In this work the basic equipment and techniques were developed which allow the sampling of lubricants from a realistic EHD point contact. Future work should be done to extend the range of the measurements made in this investigation, primarily by filling the gaps left in the energy input to the fluids. This is most easily accomplished with the hydrocarbon mixtures by varying the polymer molecular weights. With the bulk polymers, a range can be obtained by varying the experimental conditions. Other types of polymer-base oil systems need investigation.

The anomaly that occurred with the silicone fluids, i.e. the sapphire scratching while the steel sphere remained unmarred, needs an explanation.

APPENDIX A

DESCRIPTIVE DATA ON TEST FLUIDS AND ADDITIVES

Petroleum oil: R-620-12	
Source: Sun Oil Company	
Supplier's designation	R-620-12
Type	Paraffinic
Symbol used in this study	P1
Viscosity at 100°F (cs/SUS)	33.74/158.0
Viscosity at 210°F (cs/SUS)	5.402/43.95
Viscosity index (ASTM D-2270)	103
Flash point (°F)	420
Fire point (°F)	475
Pour point (°F)	5
Refractive index	1.4755
Density at 68°F (gm/cc)	0.8602
Molecular weight	404
%C atoms in aromatic rings ⁹	4.0
%C atoms in naphthenic rings ¹⁰	28.4
%C atoms in paraffinic rings ¹⁰	67.6
%C atoms in aromatic rings ¹¹	3.8
%C atoms in naphthenic rings ¹¹	27.7
%C atoms in paraffinic rings ¹¹	68.5
Average number of aromatic rings per molecule	0.18
Average number of naphthenic rings per molecule	1.66
Average number of total rings per molecule	1.84
Diester-Plexol 201 bis-2-ethyl hexyl sebacate: PL-5159	
Source: Rohm and Haas Company	
Manufacturer's designation	PL-5159
Symbol used in this study	S1
Viscosity at -65°F (cs)	7,988
Viscosity at 100°F (cs)	11.41
Viscosity at 210°F (cs)	3.32
Viscosity index (ASTM D-974)	150
Neutralization number (ASTM D-974)	0.02
Cloud point (ASTM D-2500)	below -65

Polyalkylmethacrylate Additives: PL-4521 and PL-4523		
Source: Rohm and Haas Company		
Manufacturer's designation	PL-4521	PL-4523
Percent polyalkylmethacrylate in solution	36.1	19.0
Viscosity at 210°F (cs)	796	773
Viscosity average molecular weight	560,000	1,650,000
Gel permeation chromatograph molecular weight average	828,000	1,510,000

Pentaphenyltrimethyltrisiloxane: DC-705	
Source: Dow Corning Corporation	
Manufacturer's designation	DC-705
Symbol used in this study	S5
Viscosity at 77°F (cs)	175
Density at 77°F (gm/cc)	1.09
Molecular weight	546
Flash point (°F)	470
Refractive index	1.5790

Dimethylsiloxanes: DC-200, E1923-48 and E1923-49			
Source: Dow Corning Corporation			
Manufacturer's designation	DC-200	E1923-48	E1923-49
Symbol used in this study	S6	S7	S8
Viscosity at 77°F (cs)	931	1200	1060
Molecular weight (GPC)	45,600	43,000	160,000

Modified Polyphenyl Ether: MCS-418	
Source: Monsanto Research Corporation	
Manufacturer's designation	MCS-418
Symbol used in this study	S9
Viscosity at 0°F (cs)	13,040
Viscosity at 100°F (cs)	25
Viscosity at 210°F (cs)	4.1
Viscosity at 300°F (cs)	2.0
Density at 77°F (g/ml)	1.195
Density at 100°F (g/ml)	1.184
Density at 300°F (g/ml)	1.101
Pour point (°F)	-20
Refractive index	1.6735

⁸ Calculated from viscosity data using the method of Hirschler, A. E., Journal of the Institute of Petroleum, Vol. 32, 1946, pp. 133-161.

⁹ Obtained using the Viscosity-Gravity Constant and the Refractivity Intercept using the method of Kurtz, S. S., Jr., King, R. W., Stout, W. J., and Gilbert, D. J., from a paper, "Relationship between Refractivity Intercept," presented before the Petroleum Div., ACS, September, 1955.

¹⁰Ibid.

¹¹Calculated using the n-d-M method of structural group analysis of mineral oil fractions of Van Nes and Van Westen, "Aspects of the Constitution of Mineral Oils," Elsevier Publishing Co., Inc., 1951.

BIBLIOGRAPHY

1. West, J. P., Selby, T. W., and The Dow Corning Company, "The Effect of Engine Operation on the Viscometric Properties of Multigrade Engine Oils," SAE Paper 650445, May, 1965.
2. Johnson, R. H. and Wright, W. A., "The Rheology of Multigraded Motor Oils," SAE Paper 680072.
3. Dowson, D., Higginson, G. R. and Whitaker, A. W., "Elastohydrodynamic Lubrication: A Survey of Isothermal Solutions," J. Mech. Engng. Sci., 4, No. 2, 121, 1962.
4. Crook, A. W., "The Lubrication of Rollers, III, A Theoretical Discussion of Friction and the Temperatures in the Oil Film," Phil. Trans. A254, p 237, 1961.
5. Cameron, A. and Gohar, R., "Theoretical and Experimental Studies of the Oil Film in Lubricated Point Contact," Proc. Roy. Soc. Vol. 291A, p 520, 1966.
6. Archard, B. F. and Cowking, E. W., "Elastohydrodynamic Lubrication at Point Contacts, Symp. on Elastohydrodynamic Lubrication," Proc. Inst. Mech. Engrs., 180, Pt. 3B, 47, 1965-66.
7. Crook, A. W., "The Lubrication of Rollers," Phil. Trans. A. 250, 387, 1958.
8. Archard, J. F. and Kirk, M. T., "Lubrication of Point Contacts," Proc. Roy. Soc. A 253, 52, 1961.
9. Crook, A. W., "Elastohydrodynamic Lubrication of Rollers," Nature, 190, 1182, 1961.
10. Gohar, R. and Cameron, A., "The Mapping of Elastohydrodynamic Contacts," ASLE Trans., 10, p 215-225, 1967.
11. Foord, C. A., Wedeven, L. D., Westlake, F. J. and Cameron, A., "Optical Elastohydrodynamics," Proc. Instn. Mech. Engrs., 184, Pt. 1, 1969-70.
12. Sanborn, D. M., An Experimental Investigation of the Elastohydrodynamic Lubrication of Point Contacts in Pure Sliding, Ph.D. Thesis, University of Michigan, 1969.

13. Sanborn, D. M. and Winer, W. O., "Fluid Rheological Effects in Sliding Elastohydrodynamic Point Contacts with Transient Loading: I-Film Thickness," Trans. ASME, J. Lub. Tech., 93, p 262-271, 1971.
14. Sanborn, D. M. and Winer, W. O., "Fluid Rheological Effects in Sliding Elastohydrodynamic Point Contacts with Transient Loading: II-Traction," Trans. ASME, J. Lub. Tech., 93, p 342-348, 1971.
15. Winer, W. O., et al., "Investigations of Lubricant Rheology as Applied to Elastohydrodynamic Lubrication," NASA CR 121169, Lewis Research Center, June, 1972.
16. Casale, A., Porter, R. S., and Johnson, J. F., "The Mechanochemistry of High Polymers," Rubber Chemistry and Technology, Vol. 44, No. 2, April, 1971.
17. Harrington, R. E., Zimm, B. H., "Degradation of Polymers by Controlled Hydrodynamic Shear," J. Physical Chemistry, Vol. 69, No. 1, January, 1965.
18. Porter, R. S., Klaver, R. F., and Johnson, J. F., "Recording High Shear Viscometer for Measurement at Shear Rates Near 10^6 sec⁻¹," The Review of Scientific Instruments, Volume 36, No. 12, December, 1965.
19. Porter, R. S. and Johnson, J. F., "Polyisobutene Degradation in Laminar Flow: Composition and Shear Variables," J. of Applied Physics, Vol. 35, No. 11, November, 1964.
20. Barry, A. J., "Viscometric Investigation of Dimethylsiloxane Polymers," J. of Applied Physics, Vol. 17, p 1020, 1946.
21. Wright, W. A. and Crouse, W. W., "General Relationships for Polymer-Petroleum Oil Blends," I and EC Product Research and Development, Vol. 3, p 153, June, 1964.
22. Bly, D. D., "Gel Permeation Chromatography," Science, Vol. 168, No. 3931, May, 1970.
23. Tolansky, S., An Introduction to Interferometry, Longmans, London, 1955.
24. Novak, J. D., An Experimental Investigation of the Combined Effects of Pressure, Temperature, and Shear Stress Upon Viscosity, Ph.D. Thesis, University of Michigan, 1968.

25. Van Wazer, J. R., Lyons, J. W., Kim, K. Y., and Colwell, R. E., Viscosity and Flow Measurement; A Laboratory Handbook of Rheology, Interscience, New York, 1963.
26. Adamson, A. W., Physical Chemistry of Surfaces, 2nd Ed., Interscience, New York, 1967.
27. Gunderson, R. C., Hart, A. W., ed., Synthetic Lubricants, Rienhold, New York, 1962.